Physics – Uspekhi **40** (11) 1117 – 1147 (1997)

REVIEWS OF TOPICAL PROBLEMS PACS numbers: 36.40.Vz, 36.40.Wa, **61.46.+w**, **85.42.+m**

Processes in plasma and gases involving clusters

B M Smirnov

Contents

Abstract. Peculiarities of cluster properties are considered and processes involving them discussed. Generation methods and applications in material fabrication are described. The kinetics of cluster growth in expanding vapor is analysed. The absorption and emission properties of clusters as systems of bound atoms are examined. The properties of a cluster plasma, i.e., a cluster-containing ionized gas, are discussed in relation to cluster light sources.

1. Introduction

According to the definition, clusters are systems of a finite number of bound atoms or molecules. Below we consider large clusters which are like small particles. Clusters differ from bulk small particles due to magic numbers [1 – 3]. Indeed, parameters of small bulk particles are monotonic functions of the number of atoms, while parameters of clusters have extrema at magic numbers of atoms. It means that magic numbers correspond to filled structures of clusters, in particular, to filled cluster shells. Thus a cluster containing a magic number of atoms has a higher cohesive energy, ionization potential, electron affinity etc. than clusters with numbers of atoms more or less by one.

B M Smirnov Institute for High Temperatures, Russian Academy of Sciences, ul. Izhorskaya 13/19, 127412 Moscow, Russia
Tel./Fax (7-095) 190-42 22
E-mail: smirnov@termo.msk.su

Received 30 June 1997
Uspekhi Fizicheskikh Nauk **167** (10) 1169 – 1200 (1997)
Translated by B M Smirnov

A high specific surface of clusters as small particles differs clusters from bulk systems. Various cluster parameters depend on the number of cluster atoms, so that one can adjust the parameters of bulk cluster assembled materials by the size of clusters constituting these materials. (Cluster assembled materials are fine films with embedded clusters). Note the specifics of formation and usage of clusters. A system consisting of a condensed system, gas and clusters transforms to the gaseous or condensed state under conditions of thermodynamic equilibrium in the system as follows from the concept of a critical size of the nucleation process [4 – 7]. This leads to the conclusion that the effective generation of clusters proceeds under non-equilibrium conditions, and the best way for this is the conversion of a gas or vapor in a system of clusters, i.e. this gas is transformed in a condensed phase in a space by cooling, and the process stops at an intermediate stage. The simplest way to reach it is a free jet expansion of a gas or vapor under conditions when a cluster beam is formed as a result of expansion of the gas [8 – 10]. Clusters forming in a beam are used for fabrication of fine films and cluster assembled materials. Hence cluster technology to a great degree is connected with the usage of cluster beams.

Note that cluster assembled materials are a promising direction for development in microelectronics. Indeed, a typical size for clusters consisting of hundreds or thousands atoms is several nanometers, so that the size of an individual element for an object of microelectronics can be of the order of tens nanometers. An important step in cluster technology was made as a result of the creation of the low-energy cluster beam deposition technique (LECBD) [11 – 13], so that one can expect a new advance in the fabrication of elements of microelectronics.

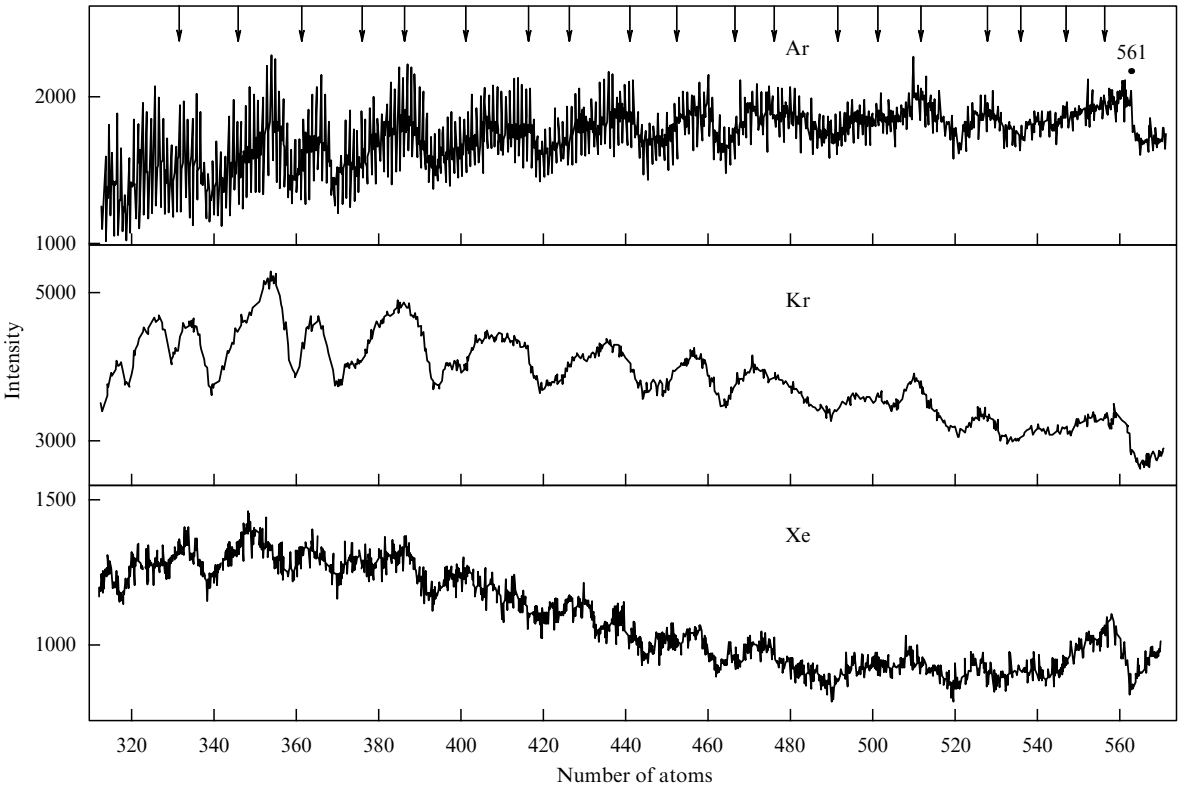

Figure 1. Mass spectra of inert gas clusters formed as a result of free jet expansion [15].

On insertion into a gas or plasma, clusters behave like small particles. In particular, at high temperatures clusters emit radiation, so that a plasma containing clusters can be a light source where clusters are effective radiators. A plasma with clusters is called a cluster plasma, and below we consider this physical object as an example of a cluster system and cluster applications.

Clusters have a high reactivity, and the contact of two clusters leads to their aggregation. Hence, in contrast to ultrafine dust [14], clusters must be isolated. Therefore, clusters are kept in beams, gases or plasmas, and have a certain lifetime. For example, the lifetime of clusters in beams is $10^{-4} - 10^{-3}$ s, the lifetime of clusters of a cluster plasma for a light source is $0.1 - 1$ s. The behaviour of clusters during their lifetime is determined by processes in which they partake. This paper is devoted to cluster processes in non-equilibrium systems and to the analysis of properties of these systems which are connected with processes involving clusters.

2. Peculiarities of cluster properties and processes

2.1 Clusters and bulk particles

Clusters as systems of bound atoms differ from macroscopic or bulk particles in the main. Indeed, any parameter of a small bulk particle, such as the binding energy, ionization potential, electron affinity, is a monotonic function of its size (or the number of atoms which constitute the particle). Clusters are characterized by so called magic numbers which correspond to extrema of these parameters. As an example, Fig. 1 shows the cluster mass dependence for the ion current in expanding inert gases. This mass spectrum reflects the size distribution of neutral clusters and shows that some numbers of cluster atoms in the distribution are preferable. These numbers do not coincide with those corresponding to the filled surface triangles of the icosahedral cluster structure which are marked in Fig. 1 by arrows. The other example of magic numbers is given in Fig. 2 where the photoionization spectrum of magnesium clusters is represented. In this case a beam of neutral magnesium clusters is intersected by a laser beam, and the forming charged clusters are detected. As is seen, the magic numbers of magnesium clusters correspond to filled icosahedral structures. These numbers are indicated in Fig. 2.

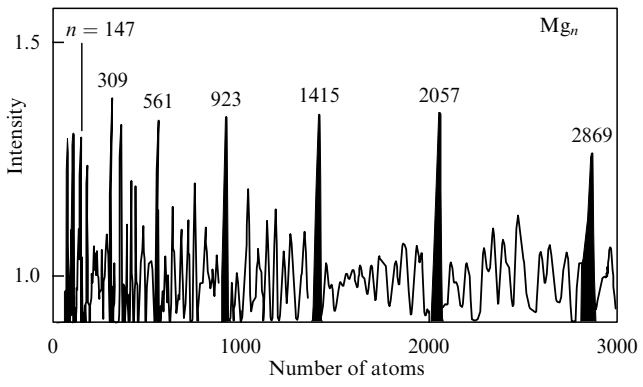

Figure 2. Mass spectra of charged Mg-clusters resulting from photoionization of a beam of neutral clusters [16].

Thus, magic numbers correspond to filled structures of clusters, i.e. filled shells or layers. The shell cluster structure relates both metallic clusters and clusters with an atomic pair interaction [17]. Clusters with magic numbers of atoms have a higher atomic binding energy, and ionization potential than clusters with neighbouring numbers of atoms. Magic numbers are observed for enough large clusters. For example, magic numbers may be extracted for clusters of alkali metals with more than 10^4 atoms [18].

Nevertheless, analyzing processes involving large clusters, we usually model clusters by bulk particles. In particular, we are guided below by the liquid drop model for a cluster, so that a cluster is assumed to be like to a liquid drop. Let us analyze the validity of such models for clusters with an atomic pair interaction. Then clusters at zero temperature have a shell structure, so that the icosahedral structure is preferable for small clusters and large clusters a the face-centred cubic structure [19–29]. Magic numbers correspond to filled shells, so that the binding energy of an atom added to a filled shell is less than that for a previous cluster. It is clear that this effect is determined by a short-range interaction because a long-range interaction is not sensitive to shell filling. Hence, this effect is stronger for clusters with an interaction between nearest neighbours.

Let us represent the total binding energy of cluster atoms in the form

$$E = \varepsilon_0 n - An^{2/3}, \tag{2.1}$$

where n is the number of cluster atoms. This formula is the expansion of the total binding energy of cluster atoms over the small parameter $n^{-1/3}$ [30]. Indeed, ε_0 is the binding energy per atom for a bulk system in the limit $n \to \infty$, A is the specific surface energy which is connected with the bulk surface tension. Tables 1 and 2 give values of these parameters for clusters of heat-resistant metals and for clusters of the first group of the periodical system of elements. These parameters follow from bulk parameters of corresponding systems [31]. The value ε_0 is taken from the dependence of the saturated vapor pressure p_{sat} on the temperature T which has the form

$$p_{\text{sat}}(T) = p_0 \exp\left(-\frac{\varepsilon_0}{T}\right). \tag{2.2}$$

Note that parameters of this formula depend both on the temperature and aggregate state of the system of bound atoms. Tables 1 and 2 give these parameters for the liquid state at the melting point. For comparison, Tables 1 and 2 contain D — the dissociation energy of diatomic A_2 [32]. Alongside it, Tables 1 and 2 contain the melting T_{m} and boiling T_{b} points of bulk metals, and the specific fusion energy ΔH_{m} [32].

Table 1. Energetic parameters of large liquid clusters of heat-proof metals.

Metal	T_{m}, K	T_{b}, K	ε_0, eV	A, eV	p_0, 10^5 atm	D, eV	ΔH_{m}, meV
Be	1560	2744	3.32	1.34	6.1	0.10	135
Ti	1941	3560	4.89	3.01	23	1.4	156
V	2183	3680	4.83	3.45	85	2.62	182
Fe	1811	3134	3.65	2.79	22	0.9	143
Co	1768	3200	3.90	2.78	31	0.9	169
Ni	1728	3186	3.16	2.62	46	1.7	182
Zr	2128	4682	6.12	3.54	64	1.5	151
Mo	2896	4912	5.78	4.24	5.7	4.1	389
Pd	1828	3236	3.67	2.68	2.7	0.76	176
W	3695	5828	8.9	4.45	22	6.9	364
Pt	2041	4100	5.6	2.20	24	0.93	207

Table 2. Parameters of bulk metals and liquid clusters of alkali metals and metals of the first group of the periodical system of elements.

Metal	T_{m}, K	T_{b}, K	ε_0, eV	A, eV	p_0, 10^5 atm	D, eV	ΔH_{m}, meV
Li	454	1615	1.61	0.99	1.3	1.05	31
K	371	1156	1.08	0.73	0.63	0.731	27
Na	336	1032	0.91	0.60	0.37	0.551	24
Cu	1358	2835	3.40	2.02	15	1.99	138
Rb	312	961	0.82	0.53	0.28	0.495	23
Ag	1235	2435	2.87	2.87	15	1.67	117
Cs	301	944	0.78	0.51	0.24	0.452	22
Au	1337	3129	3.65	2.5	12	2.31	130

For large clusters the second term of formula (2.1) is less than the first. The specific surface energy tends to constant in the limit $n \to \infty$. For finite n the function $A(n)$, which can be calculated on the basis of formula (2.1) using accurate values of E, is non-regular with an oscillating structure, so that its minima correspond to magic numbers when the binding energy of surface atoms is maximal. In the case of a short-range interaction of atoms, when only an interaction between nearest neighbours takes place in the cluster, the parameters of formula (2.1) are $\varepsilon_0 = 6$, $A(\infty) = 7.56$ [33, 34], where the dissociation energy of the corresponding classical molecule is taken as the energy unit. Figure 3 [35] confirms an oscillating structure for the specific surface energy $A(n)$. On this Figure $A(n)$ is given for large clusters with partially filled facets when the face-centred cubic structure is optimal for clusters with a short-range interaction of atoms. Then the optimal configuration of atoms for a given number of cluster atoms is taken such that it leads to a maximum binding energy. The specific surface energy is calculated from formula (2.1) on the basis of the total binding energy of cluster atoms that is proportional to the number of bonds between nearest neighbours. As is seen, if within the framework of some bulk model for a cluster we take $A(n) = \text{const}$, it leads to an error of several percent for the specific surface energy.

Thus, if a physical property or process correspond to a group of cluster sizes, and the parameter under consideration

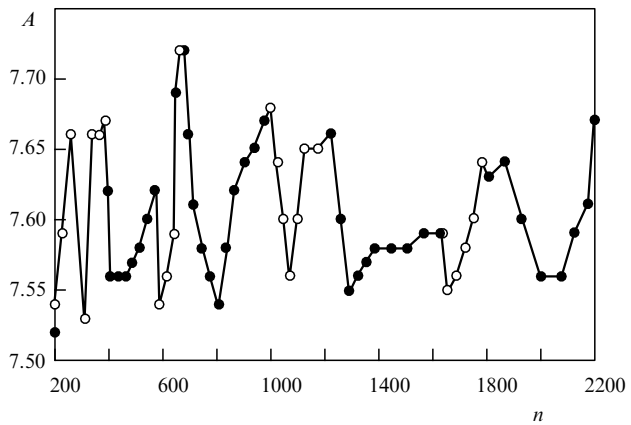

Figure 3. The specific surface energy of clusters A as a function of the number of cluster atoms n for a short-range interaction of atoms at zero temperature [35].

results from averaging over cluster sizes, it is convenient to use bulk models of clusters. In this case cluster parameters for a given size can differ remarkably from the average. Let us consider as an example the cluster cohesive energy ε_n — the binding energy of surface atoms for a cluster which is determined by the relation $\varepsilon_n = E_{n+1} - E_n$ and in the limit of large clusters has the form

$$\varepsilon_n = \frac{\mathrm{d}E_n}{\mathrm{d}n} = \varepsilon_0 - \frac{2A}{3n^{1/3}}\,, \tag{2.3}$$

where E_n is the total binding energy of a cluster consisting of n atoms.

Let us return to clusters with a short-range interaction of atoms when the binding energy of cluster atoms is proportional to a number of bonds between nearest neighbours. A new atom joined to a cluster can have the different number of bonds depending on the cluster structure at a given number of cluster atoms. Hence, the cohesive cluster energy ε_n is an irregular function of the number of atoms. As a demonstration of this fact, Fig. 4 contains the size dependence of the cohesive energy for clusters with the Lennard-Jones atomic interaction potential [36].

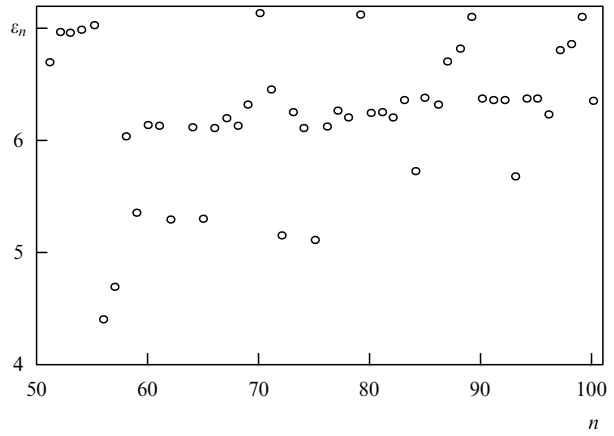

Figure 4. Binding energy of a surface atom for a cluster with the Lennard – Jones atomic interaction potential [36]. The binding energy is expressed in units of the dissociation energy of the diatomic molecule.

This analysis corresponds to zero temperature, i.e. to the ground cluster state. At high temperatures, when clusters are found in the liquid state, the size dependence of the cluster cohesive energy becomes smooth. In addition, large solid clusters become like bulk particles. The question is at which sizes and temperatures cluster properties begin to coincide with bulk ones. Under these conditions, irregular variations of the cluster energy as a function of the number of atoms due to the cluster structure are compensated by fluctuations of the energy of atom vibrations. The irregular part of the cluster energy ΔE_{ir} is the difference between the cluster energy and the smooth dependence of the cluster energy on its size constructed on the basis of accurate data at zero temperature, and can be estimated as $\Delta E_{\mathrm{ir}} \sim 10$ [37]. The fluctuation of the total cluster energy as a result of the motion of its atoms is $T\sqrt{s}$, where T is the temperature, s is the effective number of vibrations. On the basis of the Debye approximation for the cluster oscillations we have

$$s = \frac{3nT^3}{\Theta_{\mathrm{D}}^3}\,,$$

where $3n$ is the number of vibrations, so that n is the number of cluster atoms, Θ_{D} is the Debye temperature, and we assume $T \ll \Theta_{\mathrm{D}}$. Thus the criterion $\Delta E_{\mathrm{ir}} \ll T\sqrt{s}$ corresponds to the criterion that a cluster becomes a bulk particle due to the mechanism:

$$T^5 \gg T_0^5\,, \quad T_0 = \left(\frac{30\Theta_{\mathrm{D}}^3}{n}\right)^{1/5}\,. \tag{2.4}$$

Table 3 gives results of the analysis for inert gas clusters [37]. We assume that the Debye temperature of clusters coincides with that of the solid, and $\Theta_D^3 = \Theta_{\mathrm{l}}\Theta_{\mathrm{t}}^2$, where $\Theta_{\mathrm{l}}, \Theta_{\mathrm{t}}$ are the Debye temperatures for longitudinal and transverse vibrations of a solid inert gas.

Table 3. Values of the parameter T_0 for clusters of inert gases.

Metal	Parameter T_0 at	
	$n = 10^3$	$n = 10^4$
Ne	0.60	0.38
Ar	0.34	0.21
Kr	0.23	0.14
Xe	0.18	0.11

Thus, the usage of macroscopic models for clusters leads to some errors, and one can expect that if we deal with a size distribution of clusters these errors will be reduced. This can be demonstrated by measurement of the mobilities of clusters in helium [38–41]. If a cluster has a spherical form, its mobility calculated within the framework of the hard sphere model will coincide with that measured. Measurements show that it is fulfilled in most cases, but at some sizes and low temperatures the cluster shape differs from spherical. Thus the effect of the cluster structure can be essential for these clusters, but it is not strong in the case of averaging over sizes, and this effect disappears at high temperatures due to transitions of clusters of non-spherical form in excited states which have a spherical shape on average.

One more example in Fig. 5 demonstrates the difference of the form of clusters in the ground state from spherical. In this Figure the spherical coefficient ξ is taken for clusters with a short-range atomic interaction in the form

$$\xi = \frac{r_{\max} - r_{\min}}{r}\,, \tag{2.5}$$

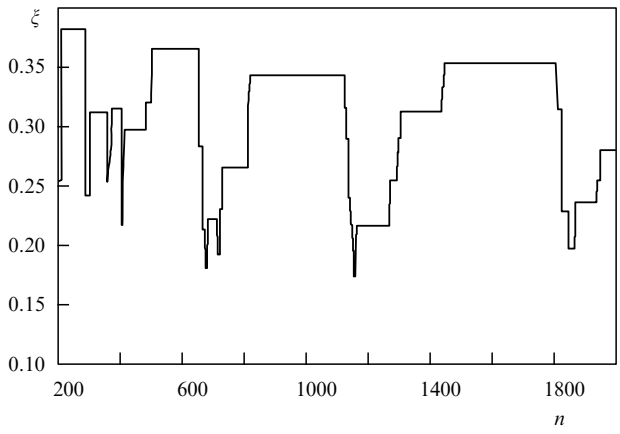

Figure 5. Sphericity coefficient ξ of solid clusters with a short-range atomic interaction with a face-centered cluster structure and a central cluster atom.

where r_{min}, r_{max} are the distances from the cluster centre of closest and farthest surface atoms, r is the cluster radius, i.e. the mean distance of surface atoms from the cluster centre. As follows from Fig. 5, the form of a solid cluster with a short-range atomic interaction differs from spherical.

2.2 Models of collisions involving clusters

Models of collision of atomic particles with a large cluster are based on the assumption that the cluster radius is larger than the radius of action of atomic forces. Then the cross section of an atom-cluster collision is

$$\sigma = \pi r^2 , \tag{2.6}$$

where r is the cluster radius. For example, if the cluster has a charge e, the cross section of the polarization capture of an atom is [42]

$$\sigma_{pol} = 2\pi\sqrt{\frac{\alpha}{2\varepsilon}}, \tag{2.7}$$

where α is the atom polarizability and ε is the collision energy. For large clusters this value is smaller than that from formula (2.6). The ratio of the cross sections (2.6) and (2.7) has the form

$$\frac{\sigma_{pol}}{\sigma} = \left(\frac{n}{n_0}\right)^{2/3} . \tag{2.8}$$

Here n is the number of cluster atoms; for example, in the case of copper $n_0 = 79$ at a temperature of 1000 K.

Formula (2.6) corresponds to the hard sphere model when a cluster is assumed to have a spherical form and the radius of action of atomic forces is small compared to a cluster radius. Below we use an additional assumption, considering a cluster to be like a liquid drop. This model is called the liquid drop model. Within the framework of this model a cluster is a drop which is cut off from the bulk liquid. Then the drop radius r and the number of cluster atoms n are connected by the relation

$$n = \frac{4\pi\varrho r^3}{3m} = \left(\frac{r}{r_W}\right)^3 , \tag{2.9}$$

where ϱ is the density of the corresponding bulk liquid, m is the atomic mass, and $r_W = [3m/(4\pi\varrho)]^{1/3}$ is the Wigner–Seitz radius. This model is convenient for the determination of averaged cluster parameters, and owing to its simplicity, it is widely used.

On the basis of formula (2.6) we have for the rate constant of atom-cluster collision

$$k = \langle v\pi r^2\rangle = \left(\frac{8T}{\pi\mu}\right)^{1/2}\pi r^2 = k_0 n^{2/3} , \tag{2.10}$$

where

$$k_0 = 1.93 T^{1/2} m^{1/6} \varrho^{-2/3} , \tag{2.11}$$

here brackets mean averaging over velocities v of colliding atomic particles, μ is the reduced atom-cluster mass which coincides with the atomic mass for a large cluster, T is the atom temperature which is expressed here and below in energetic units.

By the same way we obtain for the cross section of collision of two clusters

$$\sigma = \pi(r_1 + r_2)^2 ,$$

where r_1, r_2 is the radius of the corresponding cluster. For the liquid drop model this is the cross section for the joining of two neutral clusters, so that as a result of collision two clusters — drops join into one. The rate constant of this process is

$$k = \langle v\pi(r_1 + r_2)^2\rangle = k_0\left(\frac{n_1 + n_2}{n_1 n_2}\right)^{1/2}(n_1^{1/3} + n_2^{1/3})^2 . \tag{2.12}$$

Here v is the relative cluster velocity, μ is the reduced cluster mass, brackets mean averaging over cluster velocities, and n_1, n_2 are the numbers of cluster atoms.

Now let us consider collisions of a charged cluster with a charged atomic particle, for example, collisions of electrons or ions with a charged cluster. Then we use the relation between the impact parameter of collision ϱ and the distance of closest approach r_0 which follows from the law of conservation of the angular momentum of particles [42]:

$$1 - \frac{\varrho^2}{r_0^2} = \frac{U(r_0)}{\varepsilon} ,$$

where $U(R)$ is the interaction potential of colliding particles with a distance R between them, ε is the particle energy in the frame reference of the centre of mass. In particular, in the case of an electron collision with a cluster of a positive charge Z, we have for the collision cross section

$$\sigma = \pi\varrho^2(r) = \pi r^2 + \pi r\frac{Ze^2}{\varepsilon} , \tag{2.13}$$

where $\varrho(r)$ is the impact parameter of the collision for which the distance of closest approach r_0 is equal to the cluster radius, ε is the electron energy. These formulae will be used for the analysis of some processes and equilibria involving clusters.

Let us consider one such an equilibrium in a cluster plasma — the ionization equilibrium of clusters which is established by processes

$$A_n^Z + e \leftrightarrow A_n^{Z-1} , \tag{2.14}$$

where the subscript indicates number of cluster atoms; the superscript marks its positive charge. If we assume each contact of an electron and cluster leads to electron attachment, we can use the cross section (2.13) for electron attachment. It gives for the rate constant of electron attachment in the limit $Ze^2/r \gg T_e$:

$$k_{at} = \langle v\sigma\rangle = Ze^2\left(\frac{8\pi m_e}{T_e}\right)^{1/2} , \tag{2.15}$$

where T_e is the electron temperature and m_e is the electron mass.

Note that under the condition of the ionization equilibrium in a plasma containing electrons and charged clusters, the number densities of charged particles are connected by the Saha formula [43]

$$\frac{N_e N_{Z-1}}{N_Z} = 2\left(\frac{m_e T_e}{2\pi\hbar^2}\right)^{3/2}\exp\left(-\frac{I_Z}{T_e}\right) . \tag{2.16}$$

Here N_e is the electron number density, N_Z, N_{Z-1} are the number densities of clusters of charges Z and $Z-1$ correspondingly, and I_Z is the ionization potential of a cluster of a charge Z. On the basis of the above expression and the principle of detailed balance one can find the rate of cluster ionization in the plasma. Indeed, the ionization equilibrium in the plasma leads to the balance equation

$$N_e N_{Z-1} k_{at}(Z-1) = N_Z \nu_{ion} ,$$

where ν_{ion} is the ionization rate of a cluster by electron impact in a plasma, i.e. the number of ionization acts per cluster per unit time, $k_{at}(Z-1)$ is the rate constant of electron attachment to a cluster of a charge $Z-1$. In the limit of high electron number density it coincides with the Saha formula (2.16). Thus, we have for the ionization rate

$$\nu_{ion} = \frac{2Ze^2 r m_e^2 T_e}{\pi\hbar^3} \exp\left(-\frac{I_Z}{T_e}\right). \tag{2.17}$$

We use above the principle of detailed balance for evaluation of the ionization rate. Hence, thermodynamic equilibrium in a plasma is used only as a method, so that the ionization rate (2.17) is valid in the absence of thermodynamic equilibrium between charged particles and electrons. Next, we used the Maxwell distribution of plasma electrons for energies, i.e. an equilibrium is assumed inside the electron subsystem.

Let us consider one more problem where collisions of electrons and atoms with clusters are essential. Let the charged clusters be located in a plasma where the electron temperature T_e differs from the gaseous one T. The cluster temperature T_{cl} results from collisions of atoms and electrons with clusters. Let us use a simple model of collisions such that an atomic particle after collision obtains the cluster thermal energy on average. It means for $T_e > T$ that an atom obtains on average the energy $3(T_{cl}-T)/2$ from the cluster, and an electron transfers on average the energy $3(T_e - T_{cl})/2$ to the cluster. Then the power which a cluster takes from the electrons is $3(T_e - T_{cl})v_e N_e \sigma_e/2$, where v_e is the average electron velocity, N_e is the number density of electrons, and σ_e is the cross section of electron-cluster collisions. The power which atoms obtain from the cluster is $3(T_{cl} - T)v_a N_a \sigma_a/2$, where v_a is the average velocity of atoms, N_a is the number density of atoms, and σ_a is the cross section of collisions of atoms with the cluster. The stationary condition using formulae (2.10), (2.16) for the rate constants of collisions of atoms and electrons with clusters leads to the following expression for the cluster temperature T_{cl} [44]:

$$T_{cl} = \frac{T + \zeta T_e}{1+\zeta} ,$$

where

$$\zeta = \left(\frac{T_e m_a}{T m_e}\right)^{1/2} \left(1 + \frac{Ze^2}{r T_e}\right) \frac{N_e}{N_a} . \tag{2.18}$$

As it is seen the cluster temperature can depend both on its size and charge.

2.3 Processes of growth and evaporation of clusters in parent vapor

Now let us consider processes of evaporation and attachment of atoms to a cluster on the basis of the above formulae assuming the parameters of the cluster surface to be identical to those of the bulk one. The attachment flux for gaseous atoms to a macroscopic surface is the product of three factors

$$j_{at} = \left(\frac{T}{2\pi m}\right)^{1/2} N\xi , \tag{2.19}$$

so that the first factor is the average atomic velocity component which is directed perpendicular to the surface, m is the atom mass, N is the atom number density, and ξ is the probability of atom joining with a surface after their contact.

The flux of evaporating atoms is given by the formula:

$$j_{ev} = C \exp\left(-\frac{\varepsilon_0}{T}\right), \tag{2.20}$$

where ε_0 is the cohesive energy of a bulk surface, and parameter C depends weakly on the temperature and is determined by properties of the surface. If the atom number density is equal to the number density of saturated vapor N_{sat} at this temperature, the attachment flux becomes equal to the evaporation flux [45, 46]

$$j_{ev} = j_{at} = \left(\frac{T}{2\pi m}\right)^{1/2} N_{sat}(T)\xi ,$$

where $N_{sat}(T) = N_0 \exp(-\varepsilon_0/T)$. Thus we have for the factor in formula (2.20)

$$C = \left(\frac{T}{2\pi m}\right)^{1/2} N_0 \xi .$$

Within the framework of the liquid drop model of the cluster, we have expression (2.20) for the flux of attaching atoms. If we transit from a macroscopic surface to the corresponding cluster surface, one can use the above expression for the evaporation flux by replacing the atom binding energy ε_0 for the bulk surface for the cohesive energy of cluster atoms ε_n. Then formula (2.20) takes the form

$$j_{ev} = C \exp\left(-\frac{\varepsilon_n}{T}\right) = \left(\frac{T}{2\pi m}\right)^{1/2} N_{sat}(T)\xi \exp\left(-\frac{\varepsilon_n - \varepsilon_0}{T}\right). \tag{2.21}$$

The expressions for rate constants of processes

$$A_n + A \leftrightarrow A_{n+1} \tag{2.22}$$

involving large clusters can be obtained on the basis of formulae (2.19), (2.21). Then we transit from fluxes to the rate constants, so that the rate constant of atom attachment corresponds to formula (2.10) [45, 46]:

$$k_n = j_{at} 4\pi r^2 = k_0 n^{2/3} , \tag{2.23}$$

where k_0 is determined by formula (2.11). The rate of evaporation is connected with the rate of atom attachment by the principle of detailed balance for processes (2.22). Formula (2.23) yields the rate of cluster evaporation ν_{n+1}, i.e. the probability per unit time for evaporation of an atom from a cluster consisting $(n+1)$ atoms [45, 46]:

$$\nu_{n+1} = k_n N_{sat}(T) \exp\left(-\frac{\varepsilon_{n+1} - \varepsilon_0}{T}\right). \tag{2.24}$$

These formulae will be used for the analysis of the evolution of clusters if it is governed by processes (2.22).

2.4 Mobility and diffusion of clusters in gases

The above expressions can be used for the analysis of diffusion and the mobility of clusters in gases. First let us calculate the friction force which acts on a moving large cluster in a gas. This force results from separate collisions of atoms of a gas with the cluster, and the cluster obtains a momentum $m\mathbf{v}(1-\cos\vartheta)$ under the action of elastic scattering of an atom on the cluster, where m is the atomic mass which is significantly smaller than the cluster mass, $\mathbf{v}$ is the relative velocity of colliding particles, and ϑ is the scattering angle. Then the force acting on the cluster is

$$\mathbf{F} = \int m\mathbf{v}(1-\cos\vartheta) f(\mathbf{v}) v \, \mathrm{d}\sigma \, \mathrm{d}\mathbf{v} ,$$

where $f(\mathbf{v})$ is the distribution function of atoms on velocities which is normalized by the number density N of atoms ($\int f(\mathbf{v})\,\mathrm{d}\mathbf{v} = N$), $\mathrm{d}\sigma$ is the differential cross section of elastic scattering. The drift cluster velocity $\mathbf{w}$ is small compared to a typical atomic velocity. Taking the Maxwell distribution function of atoms on velocities $f(\mathbf{v}) \sim \exp\left[-mv^2/(2T)\right]$ and moving to the frame of reference where the mean atomic velocity is zero, we obtain using $\mathbf{v} = \mathbf{v}_\mathrm{a} - \mathbf{w}$:

$$\mathbf{F} = \int m\mathbf{v}(1-\cos\vartheta) f(\mathbf{v}_\mathrm{a}-\mathbf{w}) v \, \mathrm{d}\sigma \, \mathrm{d}\mathbf{v} = \int m\mathbf{v}\sigma^* f(\mathbf{v}_\mathrm{a}-\mathbf{w}) v \, \mathrm{d}\mathbf{v} .$$

where $\mathbf{v}_\mathrm{a}$ is mean the atom velocity. Here σ^* is the diffusion or transport cross section of atom scattered on the cluster, and for the considering model of collisions we have $\sigma^* = \pi r^2$ according to formula (2.6), where r is the cluster radius. Let us use the expansion of the Maxwell distribution function $f(\mathbf{v}_\mathrm{a}-\mathbf{w}) = f(\mathbf{v}_\mathrm{a})(1 - m\mathbf{v}_\mathrm{a}\mathbf{w}/T)$. Restricting over a cluster velocity by these expansion terms, we get for the resistance force [47]:

$$\mathbf{F} = -\mathbf{w}\frac{m^2 N\sigma^*}{3T}\langle v_\mathrm{a}^3\rangle = -8(2\pi m T)^{1/2}\frac{Nr^2\mathbf{w}}{3} , \qquad (2.25)$$

where brackets means averaging over velocities of atoms on the basis of the Maxwell distribution function of atoms.

From this one can determine the mobility of a charged cluster K which is introduced on the basis of the relation

$$\mathbf{w} = K\mathbf{E} , \qquad (2.26)$$

where $\mathbf{w}$ is the cluster drift velocity, and $\mathbf{E}$ is the electric field strength. Because the resistance force is $\mathbf{F} = Ze\mathbf{E}$ (Ze is a cluster charge), we have for the cluster mobility

$$K = \frac{3eZ}{8Nr^2(2\pi m T)^{1/2}} . \qquad (2.27)$$

From this on the basis of the Einstein relation $K = eD/T$, which connects the cluster mobility K and its diffusion coefficient in the gas D, we have in the considered case when the cluster radius r is small compared to the mean free path λ of atoms in the gas:

$$D = \frac{3T^{1/2}}{8Nr^2(2\pi m)^{1/2}} , \quad \lambda \gg r . \qquad (2.28)$$

In particular, for a particle moving in air this formula has the form:

$$D = D_0\left(\frac{a}{r}\right)^2 ,$$

where for $a = 1\mathrm{A}$ we have $D_0 = 1.6\ \mathrm{cm}^2\ \mathrm{s}^{-1}$. Note that the large clusters under consideration are small particles so that $\lambda \gg r$. In particular, for air under normal conditions it means that clusters contains less than $10^7 - 10^8$ atoms.

3. Generation of clusters

3.1 Equilibrium of clusters in the parent gas

Let us consider the character of the equilibrium of clusters in a parent vapor if they partake in processes (2.22). Then the cluster evolution of a size n is given by the balance equation

$$\frac{\mathrm{d}n}{\mathrm{d}t} = 4\pi r^2(j_\mathrm{at} - j_\mathrm{ev}) ,$$

where r is the cluster radius and $j_\mathrm{at}, j_\mathrm{ev}$ are the fluxes of atom attachment and cluster evaporation respectively. On the basis of formulae (2.19) and (2.21) one can transform this equation to the form

$$\frac{\mathrm{d}n}{\mathrm{d}t} = 4\pi r^2\frac{T^{1/2}}{(2\pi m)^{1/2}}\xi\left[N - N_\mathrm{sat}(T)\exp\left(-\frac{\varepsilon_n - \varepsilon_0}{T}\right)\right] . \qquad (3.1)$$

From this it follows that the cluster sizes are divided into two groups, so that small clusters evaporate with time, while large clusters are grown as a result of attachment of atoms. The boundary cluster size is called the critical cluster size and is determined by the relation

$$\varepsilon_n - \varepsilon_0 = T\ln S , \qquad (3.2)$$

where

$$S = \frac{N}{N_\mathrm{sat}(T)} \qquad (3.3)$$

is the supersaturation degree. Since $\varepsilon_0 > \varepsilon_n$, the critical cluster size and the above regime of cluster evolution exist only in a supersaturated vapor $N > N_\mathrm{sat}(T)$.

Let us consider the problem from another standpoint assuming the cluster equilibrium proceeds through processes (2.22). Then the size distribution function f_n of clusters satisfies the kinetic equation

$$\frac{\partial f_n}{\partial t} = Nk_{n-1}f_{n-1} - Nk_n f_n - v_n f_n + v_{n+1}f_{n+1} , \qquad (3.4)$$

where f_n is the number density of clusters contained n atoms, N is the number density of free atoms of this kind, k_n is the rate constant of atom attachment to a cluster consisting of n atoms and v_n is the rate of atom evaporation for a cluster of n atoms. Under equilibrium conditions we have

$$f_n v_n = f_{n-1}Nk_{n-1} .$$

From this it follows the relation between the equilibrium number densities of clusters of neighbouring sizes:

$$\frac{f_{n-1}N}{f_n} = N_\mathrm{sat}\exp\left(-\frac{\varepsilon_n - \varepsilon_0}{T}\right) . \qquad (3.5)$$

As is seen, this formula has the form of the Saha distribution. On the basis of formula (2.2) for the cohesive cluster energy — the binding energy of cluster atoms, we have in the limit $n \to \infty$:

$$\varepsilon_n = \frac{\mathrm{d}E_n}{\mathrm{d}n} = \varepsilon_0 - \frac{\Delta\varepsilon}{n^{1/3}} , \qquad (3.6)$$

where $\Delta\varepsilon = 2A/3$. Then using relation (3.6) in formula (3.5), one can represent it in the form

$$\frac{f_n}{f_{n-1}} = S\exp\left(-\frac{\Delta\varepsilon}{n^{1/3}T}\right). \tag{3.7}$$

Condensation of atoms takes place at $S \geqslant 1$, if the vapor density exceeds its saturation value for a given temperature. Thus, from formula (3.7) it follows that the cluster number density as a function of size has a minimum at the critical number of cluster atoms which, according to formula (3.7), has the form

$$n_{\rm cr} = \left(\frac{\Delta\varepsilon}{T\ln S}\right)^3. \tag{3.8}$$

The concept of a critical size means [4–7] that for large clusters whose size exceeds the critical one, the probability of cluster growth exceeds the probability of evaporation, and such clusters grow, whereas small clusters with $n < n_{\rm cr}$ evaporate. The critical size concept is the basis of cluster generators. As follows from formula (3.7), the number density of clusters as a function of their size has a minimum at the critical size of clusters. This leads to an important conclusion for clusters as an intermediate phase of matter between gaseous and condensed phases. According to formula (3.7), the most part of atoms of a supersaturated vapor ($S > 1$) under thermodynamic equilibrium constitute a gas or a condensed phase. It means that clusters include a small part of the atoms of a system in thermodynamic equilibrium. But transition from the gaseous to condensed phase in a space proceeds through the formation and growth of clusters. From this one can conclude that the high content of atoms in clusters corresponds to non-equilibrium conditions. Hence methods of generation of clusters are based on fast nucleation of vapors or gases in a space at the stage of violation of the thermodynamic equilibrium with a condensed phase.

For this reason, generators of clusters are usually based on their formation from a supersaturated vapor as a result of expansion of the vapor in a region of a low pressure. In the course of expansion, the vapor temperature decreases and the vapor becomes supersaturated, leading to the formation and growth of clusters or small particles. But the time of the process is not enough for the transformation of clusters in a condensed system, so that almost all the atoms of the incident vapor become clusters at the end of the process. Thus, the generation of clusters covers two stages. In the first stage of the process an atomic or molecular vapor is formed, and in the second stage this vapor is converted into a gas of clusters or a cluster beam as a result of cooling of the vapor.

3.2 Methods of cluster generation through atomic vapor

The widespread method of cluster generation uses the expansion of an atomic vapor. As a result of evolution of an expanding vapor, a cluster beam is formed. There are various methods of formation of an expanding vapor depending on the cluster material and the parameters of the final cluster beam. An oven is used for fusible metals (Fig. 6a). Then the atomic vapor formed in the oven expands through a nozzle in a vacuum together with a buffer gas. Cooling of this mixture during expansion causes nucleation of the vapor and the formation of clusters. This method generates intense cluster beams and allows clusters to be deposited onto a substratum for the production of fine films [48–71].

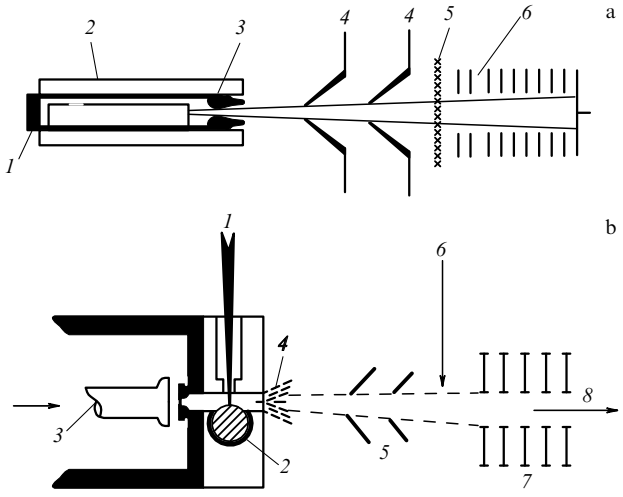

Figure 6. Schemes of cluster generation through the formation of an atomic vapor. (a) the method of heating for the creation of an atomic vapor: *1* — chamber, *2* — heater and oven, *3* — nozzle, *4* — skimmers, *5* — electron beam, *6* — accelerator and ion optics; (b) laser vaporization of metals: *1* — laser beam, *2* — rod, *3* – flow of buffer gas, *4* — beam of buffer gas and clusters, *5* — skimmers, *6* — electron beam, *7* — ion optics and accelerator, *8* — final beam.

In the case of heat-resistant metals, a laser beam is used to evaporate them and form free atoms [72–76]. Figure 6b gives a scheme of this method. Evaporated atoms are mixed with a flow of a buffer gas, and the subsequent expansion of the mixture leads to the formation of clusters. One more method of cluster formation is based on the bombardment of a target by ions of keV energies [77–87]. Then fragment-clusters formed as a result of ion impact can have a charge. They are separated and accelerated. This method allows one to obtain a beam of small clusters of low intensity and is used for the generation of selective beams of small clusters which are used for research.

The formation of clusters from an evaporating vapor can proceed in any gaseous system with a variable temperature. For example, Fig. 7 represents a scheme of a cluster lamp which will be analyzed in Section 6. Then the temperature of the buffer gas in the generation camera is significantly lower than that corresponding to the saturated vapor pressure for

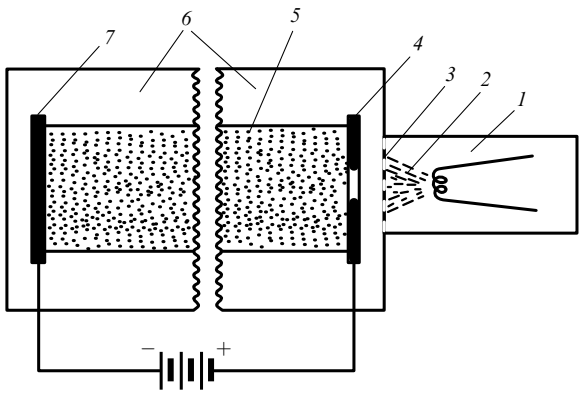

Figure 7. Scheme of a cluster lamp: *1* — chamber of cluster generation, *2* — cluster flux, *3* — grid, *4* — anode, *5* — arc discharge plasma, *6* — discharge tube, *7* — cathode.

evaporated atoms, and the formation of clusters from the vapor takes place. A typical cluster size depends on the time of cluster location in the generation chamber, so that it can be adjusted by the pressure of the buffer gas and geometry of the generation chamber. Thus, all the evaporated atoms are converted into clusters in the generation chamber, so that the energetics of the process of cluster formation are determined by the energetics of evaporation of the wire in the generation chamber. Let us analyze this process.

For definiteness, consider a tungsten wire as target for formation of atoms because it is suitable for a cluster lamp. The efficiency of formation of free atoms from this wire can be characterized by the energetic cost ε of the formation of one atom by evaporation of this wire. First we consider heating the wire by an electric current which propagates through it. Then the heated tungsten wire emits radiation like an incandescent lamp, and the atom cost is

$$\varepsilon = \frac{p}{j}\,, \tag{3.9}$$

where p is the radiation power per unit square, j is the flux of evaporated atoms. Taking these values from [31], we have a tungsten atom cost $\varepsilon = 270$ keV at $T = 3000$ K, $\varepsilon = 28$ keV at $T = 3300$ K and $\varepsilon = 4.2$ keV at $T = 3600$ K. The binding energy per tungsten atom for these temperatures is 7.9 eV [31].

One can see that heat evaporation is not a profitable method for the generation of clusters of heat-resistant metals. The sharp temperature dependence of the atom cost takes place because of the exponential temperature dependence for the evaporation flux. In the case of laser evaporation the surface temperature is higher, so that laser vaporization is more effective than evaporation of the surface by an electric current. In this respect, gas-discharge methods based on cathode sputtering by an ion current are more effective for the production of an atomic vapor which is further converted into clusters. If this process proceeds in a vacuum, an effective method results from explosive emission taking place in vacuum discharges [88, 89]. Then on the main stage of the process, an ion current vaporizes the cathode, and in this way matter is created through which the discharge current propagates. Each evaporating atom is further ionized in the plasma, so that it generates one ion and one electron. This gives a relation between the atom flux j and the discharge current density i, if we suppose the ions to be single charged

$$i = 2ej\,. \tag{3.10}$$

From this we find for the atom cost

$$\varepsilon = 2eV\,, \tag{3.11}$$

where V is the discharge drop. Usually, V is of the order of the ionization potential, i.e. $\varepsilon \sim 10$ eV. Thus, this method of creation of an atomic vapor is effective if the process proceeds in a vacuum.

For generation of atoms in a buffer gas by sputtering of the cathode it is convenient to use the magnetron discharge which is characterized by a high efficiency of cathode sputtering. Figure 8 gives a scheme of this method which uses sputtering of a cathode material in a magnetron discharge [90–92]. On the basis of this method intense beams of clusters of Ag, Al, Co, Cu, Fe, Mg, Mo, Si, Ti and TiN were produced with the mean cluster sizes of 500–10000 atoms. These charged clusters are accelerated by an external electric field which allows adjustment of the cluster energy in the range 0.1–10 eV/atom. Cluster beams are used for

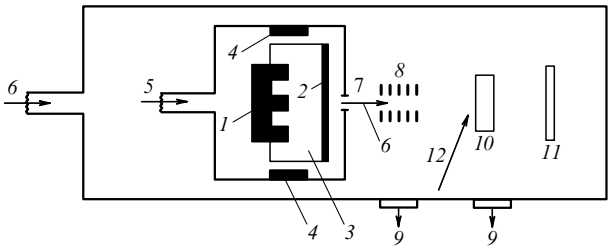

Figure 8. Scheme of a cluster generator on the basis of a magnetron discharge [90–92]: *1* — magnet, *2* — target, *3* — water cooling, *4* — electrodes, *5* — argon flow, *6* — helium flow, *7* — diaphragms, *8* — ion optics, *9* — pumps, *10* — substratum, *11* — time-of-flight mass spectrometer, *12* — Ar^+— gun for substratum cleaning.

deposition onto a substratum for fabrication of fine films, contacts and holes [90–95]. Thus, this type of gas discharge provides sputtering of electrodes and the generation of intense cluster beams. Figure 9 gives an example of the size distribution function of charged clusters and corresponds to negative copper clusters formed on the exit of magnetron gas discharge [92].

The charge of forming clusters which go through a weakly ionized gas depends on the electron temperature of the plasma (or the mean energy of electrons), and also on the electron number density. If an ionization equilibrium (2.14) is established between clusters and plasma, the relation between clusters of different charges is determined by the Saha formula (2.16). From this formula it follows that at high electron temperatures clusters are charged positively, while at low electron temperatures they can have a negative charge. In particular, let us find plasma parameters when in according with [92] 80% of clusters Cu_{1000} have a single negative charge, and 20% of clusters are neutral. Using the Saha formula (2.16) and values of the electron affinities of clusters, we find that this takes place at the electron temperature 2800 K, if the electron number density is $N_e = 10^{13}$ cm^{-3}; this corresponds

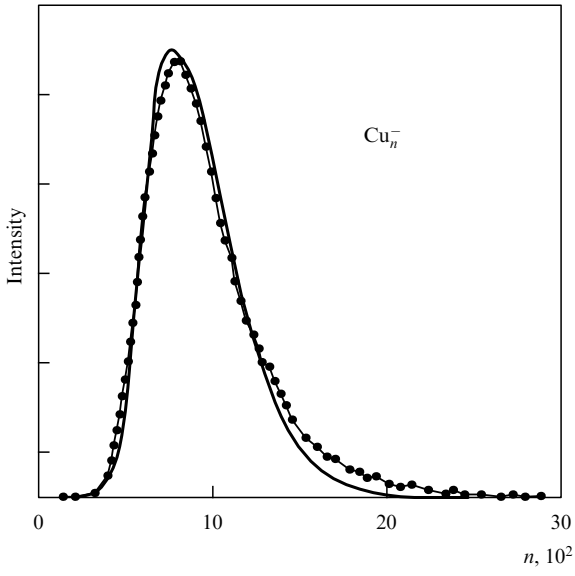

Figure 9. Size distribution function for negatively charged copper clusters generated from a magnetron gas discharge [90–92]. The solid curve corresponds to the log-normal distribution which approximates the experimental data (dots).

to a electron temperature of 2510 K, if $N_e = 10^{12}$ cm^{-3}, and the electron temperature is 2250 K for the electron number density $N_e = 10^{11}$ cm^{-3}. Note that the cluster temperature is smaller than these values of the electron temperature.

Because other types of gas discharges can be used for material sputtering, we analyze below general requirements for gas discharge with respect to generation of clusters. The first requirement relates to the effective sputtering of electrodes. Evidently, it takes place in arc discharges in regimes with formation of cathode spots. Processes in cathode spots resemble the process of explosive emission, so that a discharge electric current is concentrated in cathode spots where the current density is high enough. Then evaporation or sputtering of the cathode in cathode spots creates a region of conducting matter and provides effective propagation of an electric current. Hence, from the standpoint of gas discharge, cathode spots lead to optimal electric parameters for the gas discharge. Simultaneously, this phenomenon causes an effective erosion of the cathode material with the formation of atoms and atomic ions. It is the first stage of cluster generation.

A peculiarity of the gas discharge method for cluster generation is that clusters are not produced in the gas discharge plasma due to collision processes involving electrons and ions. Hence, the region of cluster generation must be separated from the gas discharge region. Actually, clusters are formed in the plasma afterglow where the most of plasma electrons and ions are recombined. The clusterization process proceeds at not very high temperatures and results from collisions involving evaporated atoms and atoms of a buffer gas. This process is effective at high pressures of the buffer gas, while some regimes of gas discharge require a low pressure buffer gas. Hence, it is necessary to conform the regime of a gas discharge to the parameters of the buffer gas flow. In particular, the above technique of magnetron discharge for cluster generation uses an argon pressure of 10 – 100 Pa, while the gas pressure is of the order of 1 Pa for conventional discharges of this type.

From the above analysis one can formulate general peculiarities of generators of intense cluster beams. Evidently, it is a pulse system where an atomic vapor is produced as a result of an electric breakdown with the development of cathode processes accompanied by formation of cathode spots. After the discharge is shut down, a partially ionized atomic vapor is formed. This vapor is captured by a pulse flux of a buffer gas which is conformed to the electric breakdown. In the course of propagation of the mixture formed, clusters grow and their typical sizes depend on the parameters of the mixture. In essence, this scheme of cluster generation is like that of Fig. 10 if a laser beam for evaporation of a target is changed for a pulse gas discharge as a more effective method for production of an atomic vapor. Thus, a contemporary experimental technique of generation of cluster beams uses the possibilities of processes provided by the production of clusters.

3.3 Cluster applications

Clusters have a high reactivity so that the contact of two clusters leads to their joining, and the properties of incident clusters are lost in a forming cluster. Note that in contrast to clusters, fullerenes are molecules, and the properties of individual fullerene molecules are conserved in a system of bound fullerenes owing to their closed structure. Because of their high reactivity, clusters are used in the form of a beam

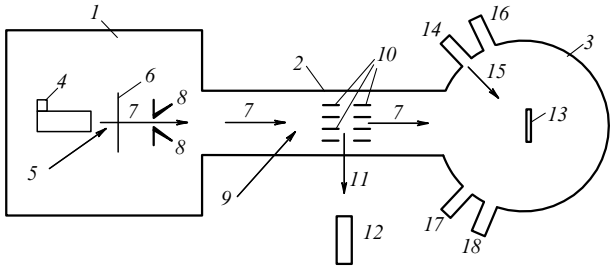

Figure 10. Scheme of the low-energy cluster beam deposition (LECBD) technique [13] for generation of a beam of neutral solid clusters and their deposition: *1* — chamber of cluster generation, *2* — tube of cluster transportation, *3* — ultra-high vacuum chamber of deposition, *4* — valve for pulse injection of helium, *5* — Ti-Sa laser beam, *6* — rod, *7* — flux, *8* — skimmer, *9* — excimer laser beam, *10* — acceleration grids, *11* — flux of detecting cluster ions, *12* — detector of cluster ions, *13* — substratum, *14* — evaporation cell, *15* — flux of matrix material, *16* — Auger spectrometer, *17* — difractometer, *18* — ion gun for cleaning of substrata.

where they are separated. There are various applications of cluster beams.

The advantage of a cluster beam consists in the possibility of charging and accelerating ions. Fast cluster ions can even be used for thermonuclear fusion reactions [96 – 100]. A convenient usage of cluster beams is connected with the fabrication of holes in foils [92]. There, each fast cluster is like a bullet, and the hole size depends on the cluster size and energy. Therefore the density and size of holes of the sieve formed can be adjusted. As a flux of energy, a cluster beam can be used for cleaning surfaces. Then surface atoms evaporate under the action of fast clusters [56, 57].

The main application of cluster beams is the fabrication of so called cluster assembled materials which have specific properties and form one of twelve existing types of nanostructures [101]. There are two methods using cluster beams. The first, the 'ion cluster beam' method [102 – 114], uses a beam of charged clusters; the scheme before deposition is shown in Fig. 6. The other method uses the low-energy cluster beam deposition (LECBD) technique [11 – 13] (see Fig. 10) and deals with a beam of neutral solid clusters of low energy. Note that fine films can be produced by other methods, while the fabrication of films with embedded solid clusters gives so called cluster assembled materials [115 – 119] which can not be formed by other methods. Below we consider the character of the interaction of a cluster beam with a substratum for each method of cluster beam deposition.

The interaction of a cluster impinged onto a film depends on the cluster energy and size (see [53, 66]). If the cluster energy is small (usually less 1 eV/atom), the cluster attaches to the surface and cluster atoms spread over the surface . In this case the cluster collides with the substratum like a liquid drop, so that on the first stage of the process a cluster attaches to the surface forming a plane contact with it. Then atoms of the outside cluster surface run over the surface due to diffusion. As a result, cluster atoms form a fine continuous film on the surface of the substratum. If the cluster energy is high, its collision with a surface causes a strong shift of the nearest surface atoms. Their motion leads to erosion and vaporization of the surface. In addition, it creates a motion of other atoms like a shock wave. Figure 11 gives an example of the development in time of a colliding cluster and surface under such conditions.

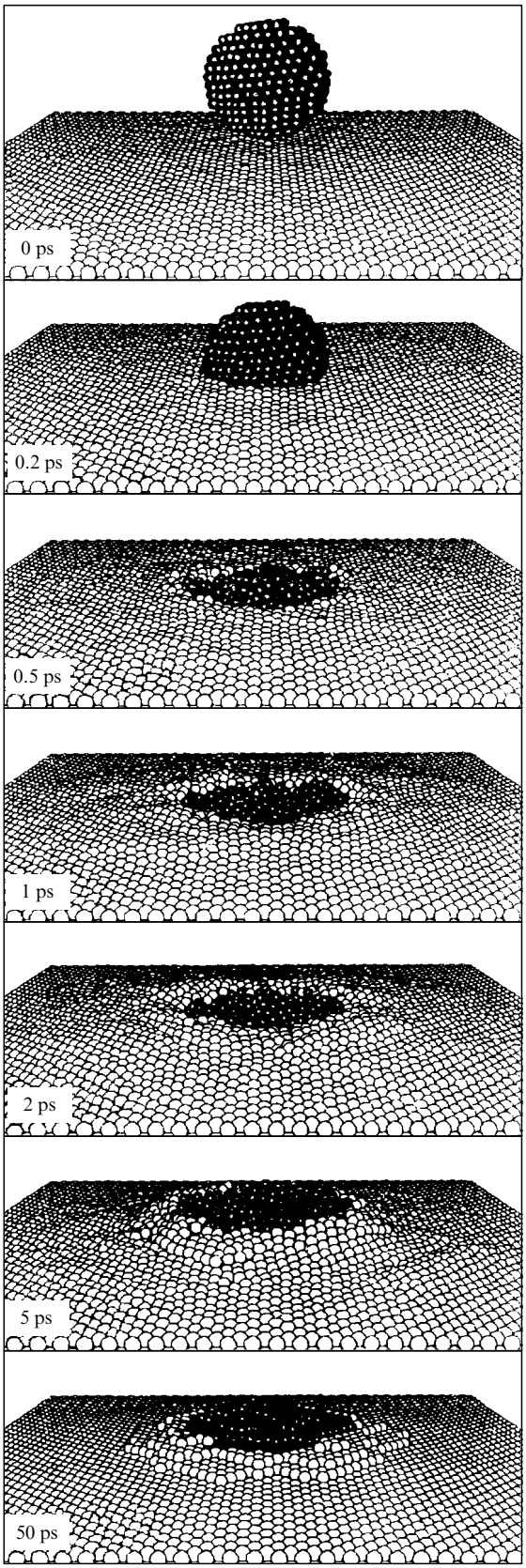

Figure 11. Series of snapshots for a collision of a Cu_{1000} cluster with a copper film according to computer simulation by methods of molecular dynamics [94, 95]. The cluster energy is 10 eV/atom, the cluster and film initial temperature is 300 K.

The ion cluster beam method is like the method of deposition by atomic beams. The maximum rate of silver deposition by the "ion cluster beam" method is 74 nm s^{-1}. An equivalent specific power more 0.2 W cm^{-2} is required for this rate of evaporation of a silver surface. Thus, an atomic beam which provides the above rate of silver deposition can be created by a laser beam of low power. This comparison shows that cluster beams lead to relatively low rates of deposition. This means that only thin films can be produced by the ion cluster beam method of deposition.

Thus, one can create more powerful atomic beams compared to cluster beams. But, there are advantages of cluster beams. First, the specific energy resulting from the joining of clusters in a bulk film is smaller than that corresponding to atoms. Indeed, the surface cluster energy is released as a result of the joining of clusters, while in the case of formation of bulk from atoms a specific bulk energy is released. In reality, these values differ by one order of magnitude. Hence, films manufactured from atoms are characterized by a higher heat tension and in the end they contain larger numbers of vacancies and strains than in the case of usage of a cluster beam.

Secondly, because clusters are charged, the energy of clusters is governed. The optimal energy of clusters for deposition is several electronvolts per atom. This energy can not be reached by a neutral atomic beam. In particular, atoms of a buffer gas at such an energy can not be inserted in the forming film. Thus, the 'ion cluster beam' method provides a higher quality of films compared to atomic beams. This method is used for the fabrication of metallic, dielectric, semiconductor and organic films, and is widely practiced in the technology of microelectronics.

The LECBD method allows one to produce cluster assembled materials which can not be manufactured by other methods. A scheme of this method is given in Fig. 10. The resulting material is a fine film of a deposited substratum with solid clusters embedded in it. These clusters can be separated on the substratum surface and can form surface fractal aggregates depending on the parameters of the deposition process and the surface density of clusters. Note that the cluster chemical structure can differ from that of bulk materials. Correspondingly, the chemical properties of films with embedded clusters can differ from the properties of bulk systems. For example [13], carbon and silicon cluster assembled films can form fullerene-like structures which include a large amount five-membered rings in a certain range of sizes of embedded clusters. Hence, the structural and chemical properties of cluster assembled materials can differ from those of bulk systems.

Films with embedded clusters can be used as filters because clusters are absorbers in a certain spectrum region. The spectral characteristics of these filters can be controlled by the sort, size and density of embedded clusters. Alongside filters, films consisting of a transparent matrix with embedded clusters can be used as elements of optoelectronics. Some transitions of clusters as atomic systems can be saturated, so that these films can be used as optical locks due to their nonlinear transparency.

Films with embedded clusters of magnetic materials (Fe, Co, Ni) are magnetic nanostructures and are like multidomain magnetic systems. In this context, the advantage of these films is as follows. Firstly, the size of individual grains of these films which coincides with the cluster size is several times less than for normal magnetic films. This fact reduces

the saturated magnetic field for this magnetic material. Secondly, the close sizes of embedded clusters which are magnetic grains increase the precision and selectivity of devices using this magnetic material. Thirdly, the possibility of using various embedded clusters allows us to create magnetic films with the given parameters. Thus, films with embedded clusters as cluster assembled materials are a new prospective material for precise technics and devices.

4. Kinetics of the clustering process

4.1 Kinetics of cluster growth in expanding vapor

The methods of cluster generation consist in the evaporation of a material and its transformation in an atomic vapor. Next, the vapor as a result of free jet expansion is transformed in a cluster beam. Below we analyze the kinetics of cluster growth in free jet expansion. There are different theoretical models for the analysis of kinetics of cluster growth in free jet expansion [119 – 124]. Below we analyze this process on the basis of transparent models [119, 121, 124] which are realistic and allow us to extract the main processes which are responsible for cluster growth. The basis of the models used is the character of the expansion process. In the course of expansion and cooling of a vapor, its temperature decreases and reaches a value when the nucleation process starts. It can proceed as a result of attachment and evaporation processes (2.22), and also by the coagulation process according to the scheme

$$\mathrm{A}_{n-m} + \mathrm{A}_m \leftrightarrow \mathrm{A}_n \,. \tag{4.1}$$

The nucleation process finishes when the density of atoms and clusters becomes small, so that collision processes cease. We account for it in the theory by the parameter τ_{ex} — the expansion time. Then the balance equation for the number density of atoms of a buffer gas N has the form

$$\frac{\partial N}{\partial t} = -\frac{N}{\tau_{\mathrm{ex}}} \,.$$

The balance equation for the total number density of vapor atoms, i.e. the number density of free and bound atoms has the same form.

Let us first consider the limiting case when the cluster growth is determined by the coagulation process (4.1). For simplicity we assume the rate constant of this process to be independent of cluster size. Then the kinetic equation for the size distribution function of clusters on a number of atoms f_n has the form

$$\frac{\partial f_n}{\partial t} = -f_n \sum_{m=1}^{\infty} k_{\mathrm{as}} f_m + \frac{1}{2} \sum_{m=1}^{n-1} k_{\mathrm{as}} f_{n-m} f_m \,,$$

where k_{as} is the rate constant of association of two colliding clusters, and the factor $1/2$ marks that the process of collisions of clusters consisting of m and $n-m$ atoms is taken into account twice. For large clusters one can replace the summation by integration, so that the kinetic equation takes the form

$$\frac{\partial f_n}{\partial t} = -k_{\mathrm{as}} f_n \int_0^{\infty} f_m \,\mathrm{d}m + \frac{1}{2} k_{\mathrm{as}} \int_0^{n} f_{n-m} f_m \,\mathrm{d}m \,. \tag{4.2}$$

Assume the buffer gas to be at rest. Then we have that the total number density of cluster atoms $N_0 = \sum_n n f_n$ is conserved during their evolution. Introduce the average size of clusters

$$\bar{n} = \frac{\sum_n n^2 f_n}{\sum_n n f_n} = \frac{\sum_n n^2 f_n}{N_n} \,. \tag{4.3}$$

The kinetic equation (4.2) has an accurate solution. Hence, the momenta $\sum_n n^k f_n$ of the distribution function can be separated. In particular, multiplying this equation by n and integrating over $\mathrm{d}n$, we obtain

$$\frac{\mathrm{d}}{\mathrm{d}t} \int_0^{\infty} n f_n \,\mathrm{d}n = -k_{\mathrm{as}} \int_0^{\infty} n f_n \,\mathrm{d}n \int_0^{\infty} f_m \,\mathrm{d}m + \frac{1}{2} k_{\mathrm{as}} \int_0^{\infty} n \,\mathrm{d}n \int_0^{n} f_{n-m} f_m \,\mathrm{d}m = 0 \,.$$

It means that the total number density of cluster atoms

$$N_0 = \int_0^{\infty} n f_n \,\mathrm{d}n$$

is conserved during cluster growth. Let us multiply the kinetic equation by n^2 and integrate over $\mathrm{d}n$. Then we obtain

$$\frac{\mathrm{d}}{\mathrm{d}t} \int_0^{\infty} n^2 f_n \,\mathrm{d}n = \frac{\mathrm{d}\bar{n}}{\mathrm{d}t} = k_{\mathrm{as}} N_0 \,.$$

From this it follows that the average cluster size varies in time according to the law

$$\bar{n} = k_{\mathrm{as}} N_0 t \,, \tag{4.4}$$

if we assume the average cluster size to be small at the beginning.

Now let us solve the kinetic equation (4.2). Let us introduce the concentration of clusters of a given size $c_n = f_n / N_0$, where N_0 is the total number density of atoms in clusters. The normalization condition for the cluster concentration has the form $\sum_n n c_n = 1$, and the kinetic equation (4.2) is

$$\frac{\partial c_n}{\partial \tau} = -c_n \int_0^{\infty} c_m \,\mathrm{d}m + \frac{1}{2} \int_0^{\infty} c_{n-m} c_m \,\mathrm{d}m \,, \tag{4.5}$$

where the reduced time is $\tau = N_0 k_{\mathrm{as}} t$. Let us take the solution of this equation in the form

$$c_n = 4\bar{n}^{-2} \exp\left(-\frac{2n}{\bar{n}}\right) . \tag{4.6}$$

This form of c_n satisfies the normalization condition $\int_0^{\infty} n c_n \,\mathrm{d}n = 1$ and gives the average value of the cluster size $\bar{n}$ in accordance with (4.4). One can see that (4.6) is the solution of equation (4.5) if $\bar{n} = \tau$ in accordance with formula (4.4), i.e.

$$c_n = \frac{4}{\tau^2} \exp\left(-\frac{2n}{\tau}\right) . \tag{4.7}$$

Evidently, solution (4.6) is valid for large τ if an initial distribution of particles by size is not essential.

The above analysis shows an instability of clusters located in some volume, so that the cluster size grows with time. If clusters are located in an expanding gas, the nucleation process finishes over a typical expansion time, so that time t in formula (4.4) must be changed for the expansion time. Let us obtain this result accurately from the kinetic equation which has the form

$$\frac{\partial c_n}{\partial t} = -\frac{c_n}{\tau_{ex}} - N_0 k_{as} c_n \int_0^\infty c_m \, dm + \frac{1}{2} N_0 k_{as} \int_0^\infty c_{n-m} c_m \, dm . \tag{4.8}$$

The first term in the right-hand side of the equation is responsible for expansion.

The character of the process is the following. In the course of expansion the rate of collision of clusters decreases, and at the end of the process the buffer gas becomes rarefied, so that collisions of clusters cease. From this one can estimate the mean size of clusters at the end of the process: $\bar{n} \sim N_0 k_{as} \tau_{ex}$.

For a more accurate determination of the mean cluster size at the end of the expansion process, let us multiply equation (4.8) by n^2 and integrate the result over dn. Using the normalization condition

$$\sum_n n c_n = \exp\left(-\frac{t}{\tau_{ex}}\right),$$

we obtain

$$\int_0^\infty n^2 c_n \, dn = \bar{n} \exp\left(-\frac{t}{\tau_{ex}}\right).$$

Thus, the above operations lead to the equation

$$\frac{d\bar{n}}{dt} = N_0 k_{as} \exp\left(-\frac{t}{\tau_{ex}}\right);$$

the solution of this equation for $t \to \infty$ is

$$\bar{n} = k_{as} N_0 \tau_{ex} . \tag{4.9}$$

The dependencies obtained give the character of connection between the parameters of the problem and the final parameters of the system. Now let us account for the size dependence of the rate constant of cluster association according to formula (2.6). Then the kinetic equation has the form

$$\frac{\partial c_n}{\partial t} = -N_0 c_n \int_0^\infty k(n,m) c_m \, dm + \frac{1}{2} N_0 \int_0^\infty k(n-m,m) c_{n-m} c_m \, dm ,$$

where N_0 is the total number density of atoms inside clusters. Multiplying this equation by n and integrating over dn, after symmetrization of the expression under the integral, if the gas is at rest we get:

$$\frac{d}{dt} \int_0^\infty n c_n \, dn = 0 ,$$

that gives $\int_0^\infty n c_n \, dn = 1$.

Multiplication of equation (4.8) by n and integration over dn leads to the following relation, if we introduce the continuous variables $x = n$, $y = m$:

$$\frac{d\bar{n}}{dt} = N_0 \int_0^\infty x \, dx \int_0^\infty y \, dy \, k(x,y) \, c_x c_y = N_0 \int_0^\infty x \, dx \int_0^\infty y \, dy \, k(x,y) \, c_x c_y (x^{1/3} + y^{1/3})^2 \frac{(x+y)^{1/2}}{x^{1/2} y^{1/2}} .$$

Above we use the relation for the rest gas $\int_0^\infty n c_n \, dn = 1$. Because of a weak dependence $k(x,y)$, one can use the above expressions for c_n in the right-hand side of the relation in the case $k = \text{const}$. Then we obtain

$$\frac{d\bar{n}}{dt} = k_0 N_0 \bar{n}^{1/6} J ,$$

where

$$J = 16 \int_0^\infty x \, dx \int_0^\infty y \, dy \exp(-2x - 2y) \times (x^{1/3} + y^{1/3})^2 \frac{(x+y)^{1/2}}{x^{1/2} y^{1/2}} = 5.54 .$$

From this follows the law of cluster growth:

$$\bar{n} = 6.3 (k_0 N_0 t)^{1.2} . \tag{4.10}$$

In the case of an expanding gas we have for the kinetic equation

$$\frac{\partial c_n}{\partial t} = -\frac{c_n}{\tau_{ex}} - N_0 c_n \int_0^\infty k(n,m) c_m \, dm + \frac{1}{2} N_0 \int_0^\infty k(n-m,m) c_{n-m} c_m \, dm .$$

Repeating the above operations, we transform this equation to integral form. Using the solution for $k = \text{const}$ in the right-hand side of the equation, we get

$$\frac{d\bar{n}}{dt} = k_0 N_0 \bar{n}^{1/6} J \exp\left(-\frac{t}{\tau_{ex}}\right),$$

where $J = 5.54$. From this we find the average size of clusters at the end of the expansion process:

$$\bar{n} = 6.3 (k_0 N_0 \tau_{ex})^{1.2} . \tag{4.11}$$

Formula (4.11) corresponds to the limiting case of a large number density of cluster atoms. Then all the vapor atoms are transformed into clusters, and because of the criterion

$$k_0 N_0 \tau_{ex} \gg 1 \tag{4.12}$$

the clusters formed are large.

In this regime of cluster growth the main time of cluster evolution proceeds according to pair processes (4.1). But in the first stage of transformation of an atomic vapor in a gas of clusters the three body process is essential which proceeds according to the scheme

$$2A + M \to A_2 + M , \tag{4.13}$$

where A is an atom of a nucleating vapor and M is an atom of a buffer gas. Correspondingly, the number density of diatomic molecules N_2 is determined by the balance equation

$$\frac{dN_2}{dt} = K N_b N^2 ,$$

where K is the rate constant of this three-body process (4.13), N_b is the number density of atoms of a buffer gas, N is the number density of a nucleating gas. We assume that starting from diatomic molecules, the cluster growth process goes as a result of pair processes (2.22), (4.1). Then the diatomic molecules forming are condensation nuclei for clusters. Below we consider the regime when process (4.13) is of importance, so that

$$KN_b N\tau_{ex} \ll 1 . \tag{4.14}$$

Then in the course of expansion of a nucleating vapor, process (4.13) delays the formation of bound systems of atoms. But the formation of diatomic molecules leads to their subsequent growth according to criterion (4.12). Let us consider the regime of cluster growth when owing to process (4.13) only a small part of the expanding vapor is transformed into a gas of clusters, but due to criterion (4.12) these clusters are large. If we neglect the detachment of molecules, the balance equation for the molecule number density has the form

$$\frac{dN_2}{dt} = KN_b N^2 - \frac{N_2}{\tau_{ex}} . \tag{4.15}$$

In the regime under consideration the number densities of atoms of a buffer gas and atoms of a vapor vary in time by the law N, $N_b \sim \exp(-t/\tau_{ex})$. Then the solution of the balance equation (4.15) has the form

$$N_2(t) = \left[1 - \exp\left(-\frac{3t}{\tau_{ex}}\right)\right] \frac{KN_b N^2 \tau_{ex}}{3} .$$

Here N_b, N are the initial number densities of atoms, N is the total number density of molecules and clusters at time t. The number of cluster atoms n is determined by the balance equation

$$\frac{dn}{dt} = k_0 n^{2/3} N .$$

Here we use formula (2.23) for the rate constant of atom attachment, neglect the process of cluster evaporation and take $\xi = 1$. Because $N \sim \exp(-t/\tau_{ex})$, the cluster size at the end of the expansion process depends on the time of formation of a diatomic molecule which is the nucleus of condensation for the cluster. The maximum cluster size corresponds to nucleation on diatomic molecules which were formed at $t = 0$ and is

$$n_{max} = \left(\frac{k_0 N\tau_{ex}}{3}\right)^3 , \tag{4.16}$$

where the atom number density corresponds to the initial time. Because of the criterion (4.12), $n_{max} \gg 1$.

Thus, in the regime of clusterization of an expanding vapor under consideration, criterion (4.14) conserves an atomic vapor from nucleation in the main, and criterion (4.12) provides large formed clusters. These criteria can be compatible if

$$N_b \ll \frac{k_0}{K} .$$

Typical values of the rate constants are $k_0 \sim 10^{-11}$ cm^3 s^{-1}, $K \sim 10^{-33}$ cm^6 s^{-1}, so that the considered regime of nucleation is valid if $N_b \ll 10^{22}$ cm^{-3}.

Let us use the connection between cluster size n at the end of the process and the time t of formation of diatomic molecules which are nuclei of condensation for these clusters. Clusters resulting from diatomic molecules which are formed at a moment t have the following size

$$n = \left(\frac{k_0 N\tau_{ex}}{3}\right)^3 \exp\left(-\frac{3t}{\tau_{ex}}\right) = n_{max} \exp\left(-\frac{3t}{\tau_{ex}}\right) ,$$

where N is the number density of vapor atoms at the initial time. Next, the number density of nucleation centres which are formed at time t is

$$\frac{dN_2}{dt} = KN_b N^2 \exp\left(-\frac{3t}{\tau_{ex}}\right) .$$

Because the cluster size n is definitively related to the time of formation of the condensation nuclei, we have from these equations for the number density f_n of clusters of a size n in the end of the process:

$$\frac{df_n}{dn} = \frac{N_{tot}}{n_{max}} , \tag{4.17}$$

where $N_{tot} = KN_b N^2 \tau_{ex}/3$ is the total number density of condensation nuclei at the end of the process, normalized to the initial time. As follows from this, the value df_n/dn does not depend on n. Besides, we know that the total number density of atoms in clusters at the end of the process is $N_{tot} n_{max}/2$. Because we assume that most atoms remain free at the end of the process, the following condition must be fulfilled instead of (4.14) ($N_{tot} n_{max} \ll N$):

$$KN_b N\tau_{ex}(k_0 N\tau_{ex})^3 \ll 1 . \tag{4.18}$$

Under these conditions, we have

$$f_n = \frac{nN_{tot}}{n_{max}} ,$$

and nf_n is the number density of atoms which are contained in clusters of size n. Then the average size of cluster formed $\bar{n}$ and the total number density of atoms in clusters are

$$\bar{n} = \frac{2n_{max}}{3} = \frac{2}{3}\left(\frac{k_0 N\tau_{ex}}{3}\right)^3 , \quad \sum_n nf_n = \frac{1}{2} N_{tot} n_{max} \ll N .$$

From the above analysis for two limiting regimes of nucleation of an expanding vapor one can conclude that criterion (4.12) is responsible for the large size of clusters formed at the end of the process. Cluster growth proceeds due to processes (2.22) when atoms of the vapor are free, and according to scheme (4.1) when these atoms are bound in clusters. Let us compare the rates of cluster growth according to processes (2.22) and (4.1).

In the regime when cluster growth is determined by attachment of free atoms to nuclei of condensation, and pair processes of cluster growth start from diatomic molecules, the average cluster size follows from formula (4.17) and is

$$\bar{n} = \frac{2}{3}\left(\frac{k_0 N\tau_{ex}}{3}\right)^3 .$$

Here N is the initial number density of nucleating atoms, and this result is valid under the condition $N \gg N_0$, where N_0 is the total number density of bound atoms in clusters.

In the other limiting case, when the cluster growth is determined by the cluster coagulation (4.1), the average cluster size is given by formula (4.11):

$$\bar{n} = 6.3(k_0 N_0 \tau_{ex})^{1.2},$$

where N_0 is the total number density of bound atoms at the beginning. This formula is valid, if the total concentration of bound atoms does not vary in the course of expansion of the gases, i.e. $N_0 \gg N$. Though these formulas correspond to different regimes of expansion, one can see from comparison of the corresponding values $\bar{n}$ that the regime of weak nucleation occurs if the expansion time τ_{ex} is small compared to a typical condensation time, i.e. a time during which all the vapor can be transformed into clusters. Formula (4.11) corresponds to the opposite relation between these times.

4.2 Peculiarities of cluster growth in vapor expansion

Let us analyze other aspects of the above regimes of nucleation in an expanding vapor. As a result of the processes of cluster growth, energy is released which leads to the evaporation of cluster atoms. Let us analyze this effect for large clusters. Using formula (2.1) for the binding energy of cluster atoms, we obtain for the released energy as a result of the process (4.1):

$$\Delta E = A\left[m^{2/3} + (m-n)^{2/3} - n^{2/3}\right], \tag{4.19}$$

where $n - m$, m are the numbers of atoms in joining clusters. In particular, for $m = n/2$, when this function of m at a given n has a maximum, formula (4.19) gives

$$\Delta E_{max} = 0.25 A n^{2/3}.$$

As is seen, this released energy is created by the surface cluster energy. Hence it is small compared with the total binding energy of cluster atoms, but it can exceed the binding energy of a surface atom.

The release of this energy leads to an increase of the temperature of the forming cluster compared to that of joining clusters. It can cause the release of surface atoms. Note that an excited cluster can emit only one atom, because evaporation of molecules and fragments is characterized by a small probability. Hence, an excited cluster resulting from joining of two clusters can subsequently emit several atoms, and we have a more complicated process compared to (4.1) which proceeds according to the scheme

$$A_{n-m} + A_m \rightarrow A_{n-q} + qA. \tag{4.20}$$

Assume that at the end of process (4.20) the temperature of a formed cluster is equal to the temperature of colliding clusters. This means that the released energy is spent on the liberation of atoms, so that the number of released atoms is

$$q = \Delta E \left(\frac{dE}{dn}\right)^{-1},$$

where dE/dn is the binding energy of surface atoms. In particular, for a large cluster we take

$$\frac{dE}{dn} = \varepsilon_0 - \frac{2a}{3n^{1/3}} \cong \varepsilon_0,$$

so that the maximum number of released atoms as a result of the formation of a cluster containing n atoms is

$$q_{max} = 0.25 \frac{A n^{2/3}}{\varepsilon_0}. \tag{4.21}$$

In particular, for a large fcc-cluster with a short-range interaction of atoms we have $q_{max} = 0.32 n^{2/3}$, for a large icosahedral cluster with a short-range interaction of atoms this formula gives $q_{max} = 0.28 n^{2/3}$, and for a large icosahedral cluster with the Lennard–Jones interaction of atoms from this formula it follows $q_{max} = 0.40 n^{2/3}$. Thus, the considered effect could be responsible for the formation of free atoms in an expanding nucleating vapor, but the number of released atoms is small compared to the number of atoms in a formed cluster.

The other peculiarity of cluster growth in free vapor expansion is connected with the size distribution function of formed clusters. Above we considered some limiting cases for cluster growth, and the size distribution function of clusters at the end of the process is a smooth function of size for these cases. Experimentally, a selectivity in the size distribution of clusters is observed. Below we consider the mechanisms creating this selectivity.

Selectivity can result from the total processes of cluster growth in the system. As an example, Fig. 9 gives the size distribution of charged copper clusters formed at the exit of a magnetron gas discharge [92]. In this case negative cluster ions are formed as a result of attachment of electrons to neutral clusters. The rate constants of these processes increases with cluster size, so that small clusters are absent in the distribution function for this case. This fact is demonstrated in Fig. 9.

The size distribution function of resultant clusters depends on their aggregate state during cluster growth. The above scheme corresponds mostly to liquid clusters with a smooth size dependence for the binding energy of cluster atoms. If growing clusters are found in the solid state, the size dependence for the binding energy of atoms is stronger and non-regular. An example of this dependence is given in Fig. 4, and jumps in the binding energy as a result of new atoms joining a cluster significantly exceeds the cluster melting point if it is expressed in energetic units.

In the course of cluster growth an equilibrium is established for clusters with neighbouring numbers of atoms. This equilibrium results for processes of atom attachment and cluster evaporation. Relation (3.7) in the case of this equilibrium has the form

$$\frac{f_n}{f_{n-1}} = S \exp\left[-\frac{\varepsilon_n - \varepsilon_{n-1}}{T}\right], \tag{4.22}$$

where ε_n, ε_{n-1} are the binding energies of atoms for clusters consisting of n and $n-1$ atoms correspondingly. For a solid cluster the exponent is large, so that the distribution function for cluster with magic numbers of atoms significantly exceeds that of clusters with neighbouring numbers of atoms. This provides the selectivity for the size distribution function of clusters.

Thus, if the cluster growth process finishes when clusters are solid, clusters are mostly formed with magic numbers of atoms. Hence, the low-energy cluster beam deposition method [13] in principle allows the generation of beams of clusters with magic numbers of atoms.

4.3 Heat processes in the nucleation of expanding vapors

The heat regime of vapor expansion is of importance for its nucleation. Indeed, the expansion process starts from high

vapor temperatures when high rates for processes of dissociation of molecules and evaporation of clusters do not allow the formation of bound atomic systems. In the course of the temperature drop resulting from the vapor expansion, these rates decrease sharply, and the nucleation process starts from some temperature. This means that in the above analysis of the clusterization process in an expanding vapor the initial number densities of atoms for the vapor and a buffer gas correspond to the temperature when the nucleation process starts. Next, the nucleation process is accompanied by an energy release which leads to heating of an expanding vapor and can prevent nucleation. Hence, the usage of a buffer gas is important. A buffer gas accelerates the processes of nucleation in the first stage and takes away an energy surplus. Below we consider the peculiarities of the heat process in the course of expansion of a nucleating vapor.

A jet expansion is an adiabatic process which is accompanies by transitions of energy between different degrees of freedom of an expanding gas. For the analysis of this process let us extract a moving gas volume V in which are located n atoms of a buffer gas and n_v atoms of vapor which consists of free atoms at the beginning. The variation of the total energy of this volume is

$$\mathrm{d}E = \mathrm{d}Q + p\,\mathrm{d}V\,,$$

where Q is the thermal energy of particles in this volume, and p is the gaseous pressure. Assuming the concentration of vapor atoms in the buffer gas to be small, we neglect the thermal energy of vapor atoms. Then the variation of the thermal energy is

$$\mathrm{d}Q = \frac{3}{2}\,n_\mathrm{b}\,\mathrm{d}T - \sum_k E_k\,\mathrm{d}n_k\,,$$

where $\mathrm{d}T$ is the temperature variation, n_k is a number of clusters consisting of k atoms and located in a given volume, and E_k is the total binding energy of atoms in a cluster containing k atoms. Introducing the number density of a buffer gas N_b and using its definition $N_\mathrm{b} = n_\mathrm{b}/V$, we obtain

$$p\,\mathrm{d}V = -n_\mathrm{b}T\frac{\mathrm{d}N_\mathrm{b}}{N_\mathrm{b}}\,,$$

where we use the equation of the gas state $p = N_\mathrm{b}T$. On the basis of the adiabatic character of the expansion process $dE = 0$, and accounting for the above relations, we obtain

$$\mathrm{d}E = \mathrm{d}Q + p\,\mathrm{d}V = \frac{3}{2}\,n_\mathrm{b}\,\mathrm{d}T - n_\mathrm{b}T\frac{\mathrm{d}N_\mathrm{b}}{N_\mathrm{b}} - \sum_k E_k\,\mathrm{d}n_k = 0\,. \tag{4.23}$$

If we neglect the nucleation process, then we get the adiabatic law of expansion of a monatomic gas

$$N_\mathrm{b} \sim T^{3/2}\,.$$

Let us assume that the flow of the buffer gas conserves a cylindrical symmetry during free jet expansion. Denote the beam radius by R and take into account that the atom flux $J = \pi R^2 N_\mathrm{b} u$ is conserved, where the drift velocity of atoms u is assumed to be independent of the temperature. Then we have $N_\mathrm{b}/N_0 = R_0^2/R^2$, where N_0, R_0 are the initial values of beam parameters. Substituting it in equation (4.22), we get

$$\frac{3}{2}\,n_\mathrm{b}\,\mathrm{d}T - 2n_\mathrm{b}\,T\frac{\mathrm{d}R}{R} - \sum_k E_k\,\mathrm{d}n_k = 0\,.$$

Now let us assume that at the beginning all vapor atoms were free, and condensation takes place in a narrow temperature range near T_*. The solution of this equation under these conditions has the form

$$T = T_*\left(\frac{R_0}{R}\right)^{4/3}\exp\frac{2\varepsilon c}{3T_*}\,, \tag{4.24}$$

where $c = n_\mathrm{v}/n_\mathrm{b}$ is the concentration of vapor atoms, ε is the cluster binding energy per atom.

From this it follows that the nucleation process does not influence the character of gas expansion if the criterion

$$c \ll \frac{T_*}{\varepsilon}$$

is fulfilled. In the opposite case, the thermal effect of the nucleation process stops this process, so that only a part of the free atoms can form clusters. For this reason a buffer gas is required for the total condensation of an expanding vapor.

Let us determined the maximum concentration of bound atoms for a pure expanding vapor. Then the released energy resulting from the formation of clusters raises the vapor temperature that stops subsequent clusterization. In this case equation (4.23) takes the following form

$$\frac{3}{2}\,n\,\mathrm{d}T - nT\frac{\mathrm{d}N}{N} - \sum_k E_k\,\mathrm{d}n_k = 0\,,$$

where n is the number of atoms in a considered expanding volume, and N, T are the number density of atoms and temperature. Let the initial values of these parameters be N_0 and T_0, and at the beginning of clusterization these values be N_* and T_*. During the first stage of expansion, when clusterization is absent, the vapor state is governed by the equation

$$\frac{3}{2}\,\mathrm{d}T - T\frac{\mathrm{d}N}{N} = 0\,,$$

so that $N \sim T^{3/2}$, and at the beginning of clusterization we have

$$N_* = N_0\left(\frac{T_*}{T_0}\right)^{3/2}.$$

At the next stage of the process $\mathrm{d}T = 0$, and we obtain

$$T\frac{\mathrm{d}N}{N} - \sum_k E_k\,\frac{\mathrm{d}n_k}{n} = 0\,.$$

The clusterization process starts at a temperature T_* when the formation of diatomic molecules — nuclei of condensation is possible. Hence, this temperature can be estimated from the relation $N_2(T_*) \sim N$, where $N_2(T_*)$ is the number density of molecules in thermodynamic equilibrium. Let us assume that the clusters forming are large, so that the binding energy per atom is close to that of the bulk which we denote by ε_0. Then the above equation of heat balance takes the form

$$\frac{3}{2}n\,\mathrm{d}T - nT\frac{\mathrm{d}N}{N} - \varepsilon_0 n\,\mathrm{d}c = 0\,,$$

where c is the concentration of bound atoms, i.e. the ratio of the number of bound atoms to the total number of atoms in a given volume.

We assume criterion (4.14) to be valid. Now it has the following form

$$KN^2\tau_{ex} \ll 1 .$$

Here K is the rate constant of the three body process $3A \rightarrow A_2 + A$, and τ_{ex} is the expansion time. If the clusterization process is limited by heat release, it proceeds at a constant temperature and leads to a maximum concentration of bound atoms at the end of the process which, according to the solution of this equation, is

$$c_{max} = \left(\frac{T_*}{\varepsilon_0}\right) \ln \frac{N_*}{N_f} , \tag{4.25}$$

where N_f is the final number density of free atoms, when the clusterization process finishes. It follows from the relation

$$kN_f\tau_{ex} \sim k_0 N_f \tau_{ex} n_{max}^{2/3} \sim n_{max} \frac{N_f}{N_*} \sim 1 ,$$

where n_{max} is a typical number of cluster atoms at the end of the process which, according to formula (4.16), is

$$n_{max} \sim (k_0 N_* \tau_{ex})^3 \sim (k_0 N_0 \tau_{ex})^3 \left(\frac{T_*}{T_0}\right)^{9/2} .$$

Thus the maximum concentration of bound atoms at the end of the expansion process of a pure atomic vapor, with accuracy up to numerical values under logarithm, is

$$c_{max} \sim \frac{T_*}{\varepsilon_0} \ln n_{max} . \tag{4.26}$$

In reality $T_*/\varepsilon_0 \sim 0.1$, so that the real maximum degree of clusterization in a pure vapor is of the order of 10%.

4.4 Gas dynamics of free jet expansion

The above analysis allows us to understand the character of cluster growth. Within the model under consideration, we use the parameter τ_{ex} as a characteristic of expansion of a nucleating vapor. It is necessary for the formation of large clusters that this time should be small compared to a typical time $(k_0 N_0)^{-1}$ of atom attachment to clusters, i.e. criterion (4.12) must be valid. When the number of nuclei of condensation is enough large under this condition, all the vapor is converted into clusters, if it does not contradict the heat balance in the system.

The expansion time τ_{ex} in the balance equations depends on the time in the general case according to the character of vapor expansion. If the nucleation process takes place in a narrow region of temperatures, this value can be taken as a constant. In order to understand the validity of this approximation, we consider below the character of gas dynamics as a result of expansion of a monatomic gas in a vacuum after a nozzle in the absence of the nucleation process.

Note that the character of vapor expansion in a vacuum depends on the nozzle profile [60, 64]. We will be guided below by the hyperbolic shape of nozzle which is more often used than others. Besides, all the expressions below correspond to monatomic gases. After a nozzle the flux obeys a directed velocity u which is given by the expression

$$u = \frac{v_0}{1 + 3/\mathrm{M}^2} . \tag{4.27}$$

Here $v_0 = (5T/m)^{1/2}$, m is the atom mass, M is the Mach number. The Mach number increase with distance from the nozzle and is large ($\mathrm{M} \gg 1$) far from it. According to Wiel [119], the dependence of the Mach number on the distance x from a nozzle is given by the formula

$$\mathrm{M} = 1 + 2.82\delta \tan\alpha , \tag{4.28}$$

where $\delta = x/d$, d is the nozzle diameter, 2α is the total opening angle of the nozzle. This formula is valid up to $\delta = 15$. At larger distances one can use the Hagena asymptotic expression [59]

$$\mathrm{M} = 2.72\delta^{2/3} . \tag{4.29}$$

The dependence of parameters of an expanding vapor on the distance from a nozzle can be expressed through the Mach number. In particular, in the absence of condensation the vapor temperature is [125]

$$T = \frac{T_0}{1 + \mathrm{M}^2/3} . \tag{4.30}$$

Using it in equation (4.23) for the gaseous temperature, one can obtain values of τ_{ex} over a wide range of distances after the nozzle. One more peculiarity of the expansion process consists in the violation of formula (4.29) at very large δ. The Mach number and the gaseous temperature at infinite values of δ tend to finite values [125]. It may be of importance for the condensation process, because this fact changes the character of the process.

A convenient scaling law for vapor parameters during a free jet expansion was suggested by Hagena [61]. The basis of this procedure is such that on the basis of three gaseous parameters one can construct the reduced parameters of a gas and by these reduced parameters one can describe the evolution of the gas. As gaseous parameters, Hagena took the binding energy of bulk per atom ε, the bulk density ϱ and the atom mass m. Taking these into account and using experimental data, Hagena [61] chose combinations of parameters through which one can express characteristics of condensation for various gases and vapors. One such parameter is

$$\psi_* = \frac{\psi}{\psi_{ch}} , \qquad \psi_{ch} = N_0 d T_0^{-1.25} . \tag{4.31}$$

Here N_0 is the initial number density of atoms, T_0 is the initial temperature, and d is the nozzle diameter. The parameter ψ_{ch} is constructed from the above parameters of the gas and is 1.7×10^{11} cm^{-2} K$^{-1.25}$ for argon, and 3.3×10^9 cm^{-2} K$^{-1.25}$ for copper. The parameter ψ determines the final gaseous temperature after a nozzle T_∞ which is [61]

$$T_\infty = 0.6 T_{ch} (\psi_*)^{-0.8} , \tag{4.32}$$

where T_{ch} characterizes the binding energy of large clusters. This value is $930\,K$ for argon and 4.06×10^4 K for copper. These relations are convenient for the analysis of the condensation process.

For a demonstration of use of the above relations let us analyze the character of condensation of copper under the conditions of the experiment [126]. In this experiment the condensation of copper up to the formation of dimers was

studied. The initial vapor temperature was $T_0 = 2500$ K, the initial vapor pressure was $p_0 = 100$ Torr, and the nozzle diameter $d = 0.625$ mm. These parameters correspond to a final temperature of the copper vapor $T_\infty = 330$ K. One can consider that the temperature when the condensation starts coincides with the vibrational $T_{\rm vib}$ or rotational $T_{\rm rot}$ temperatures of dimers when their concentration is small. According to the above experiment for copper, these parameters are [126] $T_{\rm vib} = 950 \pm 100$ K, $T_{\rm rot} = 800 \pm 50$ K. From formula (4.24) it follows that due to the condensation process the final temperature increases up to $T_{\rm min}$ which is given by the expression

$$T_{\rm min} = T_\infty \exp\frac{2\varepsilon c}{3T_*} . \tag{4.33}$$

From this it follows that the maximum concentration of dimers at the end of the process at the temperature $T_* = T_{\rm min}$ satisfies the relation

$$c < \frac{3T_*}{2\varepsilon} \ln\frac{T_*}{T_\infty} \tag{4.34}$$

and in this case ε correspond to the dissociation of the diatoms. The above data and formulas give $c = 5-7\%$ for the maximum diatomic concentration in this case.

The above model with the parameter $\tau_{\rm ex}$ which characterizes the expansion process is valid if the clustering process proceeds in a small space region. According to research for free jet expansion in monatomic gases, it is not fulfilled in reality. Hence, for a numerical analysis of the nucleation process in a free jet expansion, it is necessary to account for the gas dynamics of a flux after a nozzle. Note that the information used corresponds to a vapor expansion without nucleation. But because the nucleation process influences the flux temperature, it changes the gas dynamics of an expanding beam. Thus, the correct solution of the problem of nucleation in free jet expansion of a vapor requires taking into account the processes of cluster growth together with the heat balance of a nucleating beam and its gas dynamics. The above model of these processes allows us to understand the qualitative character of nucleation processes and the dependence of the size distribution function of the clusters formed on the parameters of the system.

5. Radiative processes involving clusters

5.1 Absorption cross section of bulk particle

Clusters are effective radiators, and their presence in a hot or weakly ionized gas may be important for the radiative parameters of these systems. Below we will be guided by metallic clusters where this effect is strong. For example, take an alkali metal atom which has strong resonant spectral lines of absorption. When we join atoms of an alkali metal in a cluster, these spectral lines are converted into spectral bands located in the visible range of the spectrum or the adjacent infrared and ultraviolet ranges of the spectrum. A hot cluster emits radiation in this spectrum range like a hot surface, but with a higher efficiency. In addition, such a cluster is transparent for hot infrared radiation, so that it is an effective light radiator. Note that the recombination radiation of a gas discharge plasma, which determines the radiative parameters of gas discharge sources of light, results from collisions of electrons and ions, i.e. it is a secondary process in the system. A system with hot clusters is an effective source of light because the radiation of a hot cluster is the primary process. Thus, radiative properties of metallic clusters require special analysis.

Let us find the expression for the absorption cross section of a small particle whose size r is small compared to the wavelength λ:

$$\lambda \gg r . \tag{5.1}$$

In this case the interaction potential of the electromagnetic wave and particle is $-\mathbf{ED}$, where $\mathbf{E}$ is the electric field strength of the wave, and $\mathbf{D}$ is the dipole moment induced on the particle by the electromagnet wave. The power absorbed by the particle is:

$$P = -\left\langle \mathbf{E}\frac{{\rm d}\mathbf{D}}{{\rm d}t} \right\rangle$$

where the brackets mean averaging over time. Let us take the electric field strength of a monochromatic electromagnetic wave in the form

$$\mathbf{E} = \mathbf{E}_0 \exp({\rm i}\omega t) + \mathbf{E}_0^* \exp(-{\rm i}\omega t) ,$$

where ω is the wave frequency. For the induced dipole moment by the electromagnetic field it gives:

$$\mathbf{D} = \alpha(\omega)\mathbf{E}_0 \exp({\rm i}\omega t) + \alpha^*(\omega)\mathbf{E}_0^* \exp(-{\rm i}\omega t) ,$$

where $\alpha(\omega)$ is the particle polarizability. From this it follows for the absorbed power

$$P = {\rm i}\omega |E_0|^2 (\alpha^* - \alpha) .$$

The energy flux for this electromagnetic wave is $J = c|E_0|^2/(2\pi)$. Thus, the absorption cross section of the particle as the ratio of the absorber power to the energy flux for the electromagnetic wave is [127]

$$\sigma_{\rm abs} = \frac{P}{J} = 4\pi\frac{\omega}{c} \,{\rm Im}\,\alpha(\omega) . \tag{5.2}$$

The deduction of this formula is made in order to understand the criteria of its validity. As is seen, formula (5.2) is based on assumption (5.1). If we use the expression for the polarizability α of a small spherical particle [127], we obtain for the absorption cross section:

$$\sigma_{\rm abs}(\omega) = \frac{12\pi\omega}{c} \frac{\varepsilon''}{(\varepsilon'+2)^2 + (\varepsilon'')^2} r^3 = \frac{12\pi\omega}{c} r^3 g(\omega), \tag{5.3}$$

where r is the particle radius, the dielectric constant of the particle material is taken in the form $\varepsilon(\omega) = \varepsilon'(\omega) + {\rm i}\varepsilon''(\omega)$, and

$$g(\omega) = \frac{\varepsilon''}{(\varepsilon'+2)^2 + (\varepsilon'')^2} .$$

As is seen, the absorption cross section $\sigma_{\rm abs} \sim (r/\lambda)r^2$, i.e. is small compared to the particle cross section πr^2.

Note that formula (5.2) does not connect with the Mie theory [128] of scattering of an electromagnetic wave on a bulk particle. This theory requires the macroscopic character

of refraction of an electromagnetic wave when it goes through the boundary of a bulk system. These conditions may be violated for small particles, and formulae (5.2) and (5.3) are based on other criteria. We deduced these formulae in order to convince the reader of this fact.

Let us use the Drude–Sommerfeld theory [129, 130] for metallic particles interacting with electromagnetic waves. Then electrons of the particles are like a gas of free classical electrons, so that for the dielectric constant of this electron gas we have

$$\varepsilon(\omega) = 1 - \frac{\omega^2}{\omega_p^2} . \tag{5.4}$$

Here $\omega_p = (4\pi N_e e^2/m_e)^{1/2}$ is the plasma or Langmuir frequency, so that N_e is the electron number density, e, m_e is the electron charge and mass correspondingly. Damping of plasma waves determines the imaginary part ε'' of the dielectric constant. The assumption $\varepsilon'' \ll 1$ transforms formula (5.3) with usage (5.4) to the following form in the vicinity of the resonant frequency:

$$\sigma_{abs}(\omega) = 2\pi \frac{\hbar\omega^2}{c} r^3 \frac{\Gamma}{\hbar^2(\omega-\omega_0)^2 + \Gamma^2} = \sigma_{max} \frac{\Gamma^2}{\hbar^2(\omega-\omega_0)^2 + \Gamma^2} , \tag{5.5}$$

where $\omega_0 = \omega_p/\sqrt{3}$ is the resonant frequency, $\Gamma = \hbar\omega_0\varepsilon''/6$ is the resonance width, and σ_{max} is the maximum absorption cross section:

$$\sigma_{max} = \frac{2\pi\hbar\omega_0^2 r^3}{\Gamma c} . \tag{5.6}$$

From formula (5.5), the integral relation follows as

$$\int \sigma_{abs}(\omega)\, d\omega = \pi\sigma_{max} \frac{\Gamma}{2\hbar} , \tag{5.7}$$

where the resonance width is assumed to be relatively small. Within the framework of the liquid drop model for a metallic particle, we have $r^3 = r_W^3 n$, where r_W is the Wigner–Seitz radius, and n is the number of particle atoms. One can conclude from formula (5.5) that the absorption cross section is proportional to the number of particle atoms.

5.2 Absorption of clusters

Though the above description of a bulk particle is rough for clusters, it includes the principal mechanism of metallic clusters with an electromagnetic wave through valent electrons. Hence, the absorption spectrum of metallic clusters is concentrated in the visible range of the spectrum or near it, and absorption in farthest infrared spectrum range is absent. In reality, the absorption spectrum of metallic clusters can have a more complex structure and include several maxima. Table 4 contains parameters of the absorption cross section of metallic clusters for elements when the spectrum consists of one bell-like curve. These cross sections are measured in [131] for silver, [132, 133] for potassium and [134] for lithium. The basis of measurement of the absorption cross section of metallic clusters is the concept of photoinduced evaporation [135], so that the absorption of photons leads to cluster fragmentation. Then measurement of the size distribution function of cluster ions as a function of the intensity of incident laser beam at a given geometry of the experiment allows us to find the absorption cross section. Below we will use the data of Table 4 as model values for the calculation of the radiation parameters of clusters located in a hot gas or plasma. In some cases the absorption cross section as a function of the photon energy do not have a plasmon-like form. As an example, Fig. 12 gives the absorption cross sections for some clusters Ag_n [135] which show that the spectrum form of clusters can be different. The other example corresponds to Na_n clusters [136] when the absorption spectrum has a more complex form than in the plasmon case.

Table 4. Parameters of the absorption cross sections for metallic clusters.

Cluster	$\hbar\omega_0$, eV	Γ, eV	σ_{max}, Å^2	ξ	β	f
Li_{139}^+	2.92	0.90	62	2.8	0.24	0.58
Li_{270}^+	3.06	1.15	120	3.2	0.30	0.73
Li_{440}^+	3.17	1.32	280	4.9	0.50	1.20
Li_{820}^+	3.21	1.10	440	3.3	0.52	0.85
Li_{1500}^+	3.25	1.15	830	3.5	0.66	0.91
K_9^+	1.93	0.22	26	2.9	0.27	0.91
K_{21}^+	1.98	0.16	88	2.9	0.52	0.96
K_{500}^+	2.03	0.28	1750	4.0	1.3	1.40
K_{900}^+	2.05	0.40	2500	4.5	1.2	1.59
Ag_9^+	4.02	0.62	8.84	2.6	0.24	0.87
Ag_{21}^+	3.82	0.56	16.8	2.1	0.26	0.64

From Table 4 it follows that parameters of the absorption cross-section in formula (5.5) weakly depend on the cluster size. Below we use average values of these parameters. The statistical treatment of experimental data for cluster ions Ag_9^+ and Ag_{21}^+ [131] gives $\hbar\omega_0 = 3.9 \pm 0.1$ eV, $\Gamma = 0.59 \pm 0.03$ eV, $\sigma_{max}/n = (9 \pm 1) \times 10^{-17}$ cm^2, for cluster ions $K_9^+ - K_{900}^+$ [132, 133] it yields $\hbar\omega_0 = 2.00 \pm 0.05$ eV, $\Gamma = 0.26 \pm 0.10$ eV, $\sigma_{max}/n = (34 \pm 6) \times 10^{-17}$ cm^2, and for ion clusters $Li_{139}^+ - Li_{1500}^+$ [134] these parameters are $\hbar\omega_0 = 3.1 \pm 0.1$ eV, $\Gamma = 1.12 \pm 0.15$ eV, and $\sigma_{max}/n = (52 \pm 8) \times 10^{-17}$ cm^2. In Table 4 we compare the maximum absorption cross section with the cluster section $\pi r^2 = \pi r_W^2 n^{2/3}$, where r is the cluster radius, and r_W is the Wigner–Seitz radius. The ratio of these values is

$$\beta = \frac{\sigma_{max}}{\pi r_W^2 n^{2/3}} . \tag{5.8}$$

Value β is given in Table 4. Because $\sigma_{max} \sim n$, this ratio grows with increasing cluster radius.

Note that the plasmon mechanism of absorption leads to relation (5.6) for the maximum absorption cross section. One can check the validity of this relation for measured parameters of the absorption cross section. Let us introduce the parameter

$$\xi = \sigma_{max} \frac{\Gamma c}{2\pi\hbar\omega_0^2 r^3} ,$$

which is equal to unity if formula (5.6) is valid. Values of these parameters for metallic clusters with the plasmon-like form of absorption cross section are given in Table 4. As is seen, parameter ξ differs from unity stronger than follows from the accuracy of the parameters used. It means that the assumptions used are not valid. These assumptions are based on the bulk nature of absorption that is expressed by formula (5.3) and on the plasmon character of the interaction of an electromagnetic wave with cluster valent electrons that leads to formula (5.4). Thus we conclude that the concept of

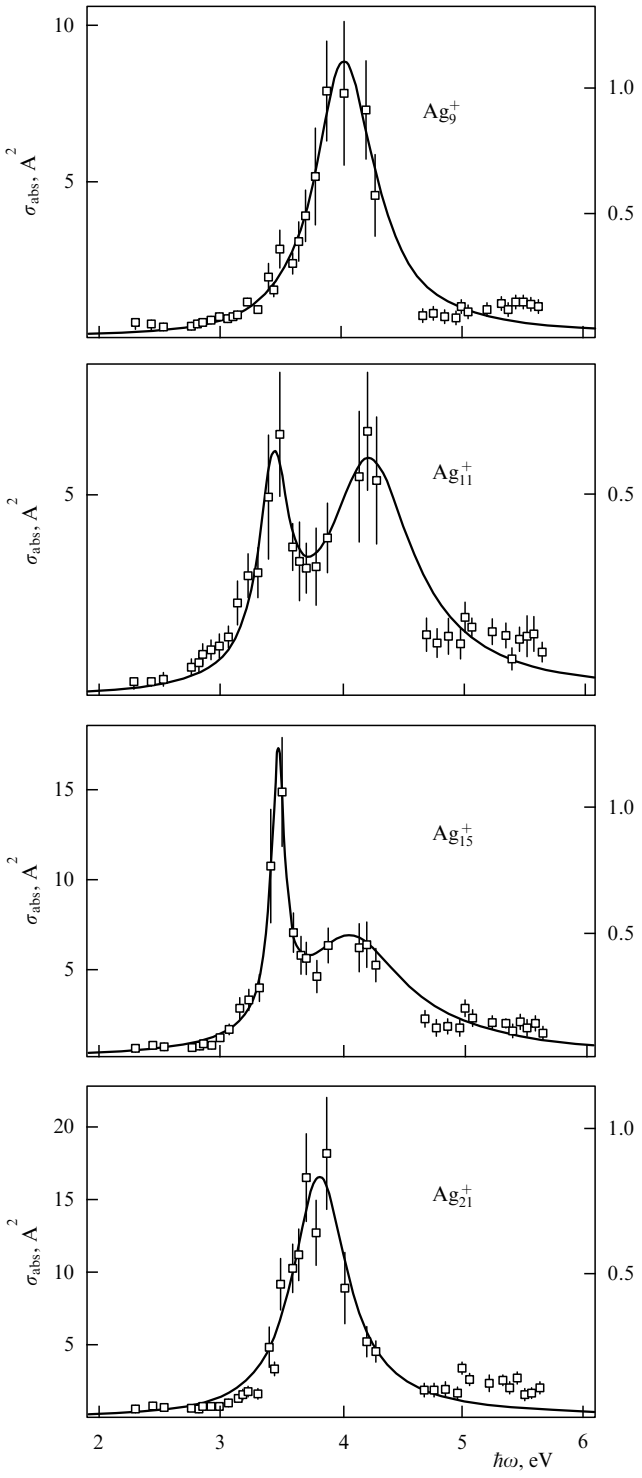

Figure 12. Absorption cross section of silver cluster ions [131].

absorption of an electromagnetic wave by a metallic cluster as a result of the interaction of the wave with a bulk plasmon is not valid even in cases when the spectral form of the absorption cross section corresponds to the plasmon case.

One more comparison confirms this conclusion. The resonant frequency for the plasmon character of the interaction of an electromagnetic wave with a metallic cluster is

$$\omega_0 = \omega_p\sqrt{3} = \frac{3e}{m_e^{1/2} r_W^{3/2}}\,,$$

because the number density of valent electrons is $N_e = 3/(4\pi r_W^3)$, where e, m_e are the electron charge and mass, and r_W is the Wigner – Seitz radius. From this formula it follows that $\hbar\omega_0 = 13.5$ eV for large lithium clusters, $\hbar\omega_0 = 7.1$ eV for large potassium clusters and $\hbar\omega_0 = 14.7$ eV for large silver clusters. A strong deviation of these values from the data of Table 4 convinces us that the bulk plasmon model is not valid for these metallic clusters.

Let us consider the sum rule for a metallic cluster. We use that for fixed nuclei the cluster spectrum in the considered spectrum range consists of a finite number of 'stocks' comparable with the number of cluster atoms. In the limit of one atom this spectrum is converted into one or several resonant spectral lines of this atom. Let us introduce the effective oscillator strength f per valent electron, so that the sum of oscillator strengths of this stock form spectrum is nf, where n is the number of valent electrons of cluster atoms. As a result of motion of cluster nuclei, the cluster spectrum becomes continuous with several maxima, but the sum rule is conserved. Below we consider the sum rule in the case when the cluster spectrum has a plasmon-like form, as takes place for clusters of Ag, Li, K of Table 4.

Let us use a general formula for the absorption cross section of an atomic system [137]:

$$\sigma_{abs}(0 \to k) = \frac{\pi^2 c^2}{\omega^2}\,\frac{a_\omega}{\tau_{0k}}\,\frac{g_k}{g_0} = \frac{2\pi^2 c^2}{m_e e}\, f_{0k} g_k a_\omega\,. \tag{5.9}$$

Here m_e is the electron mass, ω is the frequency of the considered electron transition between states 0 (lower state) and k (upper state), g_0, and g_k are the statistical weights of the transition states, τ_{0k} is the radiative lifetime with respect to this transition, and a_ω is the frequency distribution function of radiative photons, so that $\int a_\omega\,\mathrm{d}\omega = 1$, f_{0k} is the oscillator strength for a given transition, so that the sum rule for dipole radiative transitions of valent electrons for a spectrum range included resonant transitions has the form:

$$\sum_k f_{0k} = nf.$$

For definiteness, we consider clusters consisting of atoms with one valent electron, as the clusters of Table 4. Then, assuming the considered range of the spectrum to include all the resonant dipole transitions of electrons, integrating over frequency in the vicinity of each cluster resonant transition and summarizing over all the resonant transitions, we obtain the following integral relation for the absorption cross section:

$$\int \sigma_{abs}(\omega)\,\mathrm{d}\omega = \frac{2\pi^2 e^2}{m_e c}\, nf. \tag{5.10}$$

If the absorption cross section of clusters has a plasmon-like form, as the elements of Table 4, the sum rule (5.7) is fulfilled. Then from formulae (5.7) and (5.10) it follows

$$f = \frac{\sigma_{max}\Gamma m_e c}{4\pi e^2 n\hbar}\,. \tag{5.11}$$

Table 4 contains the values of the oscillator strength f of metallic clusters per valent electron when the absorption spectrum can be approximated by a plasmon-like resonance. There is an excess of these values for each element that could be connected with the restricted accuracy of the data used. On

average, the values of f for each element correspond to the oscillator strength of the lowest resonant transition $^2S_{1/2} \rightarrow {}^2P_{1/2}$, $^2P_{3/2}$ of the corresponding atom. These atomic oscillator strengths are [138] 0.74 for lithium, 1.05 for potassium and 0.77 for silver. The coincidence of the cluster and atom oscillator strengths confirms the concept that the active spectrum of metallic clusters is a result of the transformation of atomic resonant spectral lines by means of atom interactions. Thus, one can consider radiative transitions in clusters as individual radiative transitions for valent electrons in this system of bound atoms, and these transitions are broadened due to the motion of nuclei.

From the above data one can conclude that there is a partial analogy of valent electrons of metallic clusters with free electrons of a plasma. This analogy means that only electrons are responsible for the interaction of the atomic system with an electromagnetic wave in both cases. The character of the radiation of metallic clusters as systems of bound atoms with interacting valent electrons can be considered in the following way. Let an individual atom have a resonant excited state, so that a dipole radiative transition connects this state with the ground state. Usually, the lowest resonant atom state is characterized by the maximum oscillator strength for a transition from the ground state. Now compose a cluster from n atoms. If the positions of the atomic nuclei are fixed, the atomic resonance spectral line is split into n lines. Due to vibrational motion of nuclei in a solid cluster, these lines are broadened and partially overlap. Hence, the absorption spectrum of a metallic cluster contains several (or one) wide resonances. This form of absorption spectrum of metallic clusters is taken into account in calculations of the maximum absorption cross-sections of clusters (for example, [139–146]). Note that from this consideration relationship (5.10) follows. It gives that the absorption cross section of a cluster is proportional to the number of cluster atoms. The same dependence follows from a bulk model of clusters (5.3), though the above analysis leads to the conclusion that this model is not valid for metallic clusters.

As an example of such a behaviour of the cluster absorption spectrum, let us considered the mercury clusters studied in [147, 148]. Figure 13 explains the character of the transition from the absorption spectrum of a mercury atom to bulk mercury through clusters. Valent electrons of the ground state of a mercury atom are found in electron shells $6s^2$ and $5d^{10}$, so that the main resonant atomic transition is $6s \rightarrow 6p$ and an additional resonant transition is $5d \rightarrow 6p$. As mercury atoms join in a cluster, the resonant spectral lines are broadened, so that two spectral lines of the mercury atom are converted into two spectral bands of a cluster. Figure 14 proves this conclusion for large cluster ions. It shows that the absorption spectrum of mercury cluster ions consists of two bands.

According to the above consideration, the broadening of spectral lines of a cluster is determined by motion of nuclei. Hence, the spectra of solid and liquid clusters can be different, so that the spectrum of solid clusters has a more complex structure. This is demonstrated in Fig. 15 [149] where the absorption cross-section for cluster ions Na_{11}^- is given at different temperatures. As follows from this figure, individual bands in the absorption spectrum are broadened with increase of the temperature and can overlap. Hence, the form of the absorption spectrum is simplified with increasing temperature. This effect also corresponds to other cluster

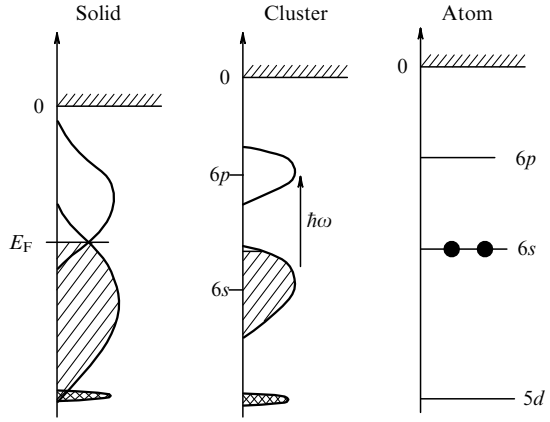

Figure 13. Radiative transitions in a mercury atom, mercury cluster and bulk mercury [147, 148].

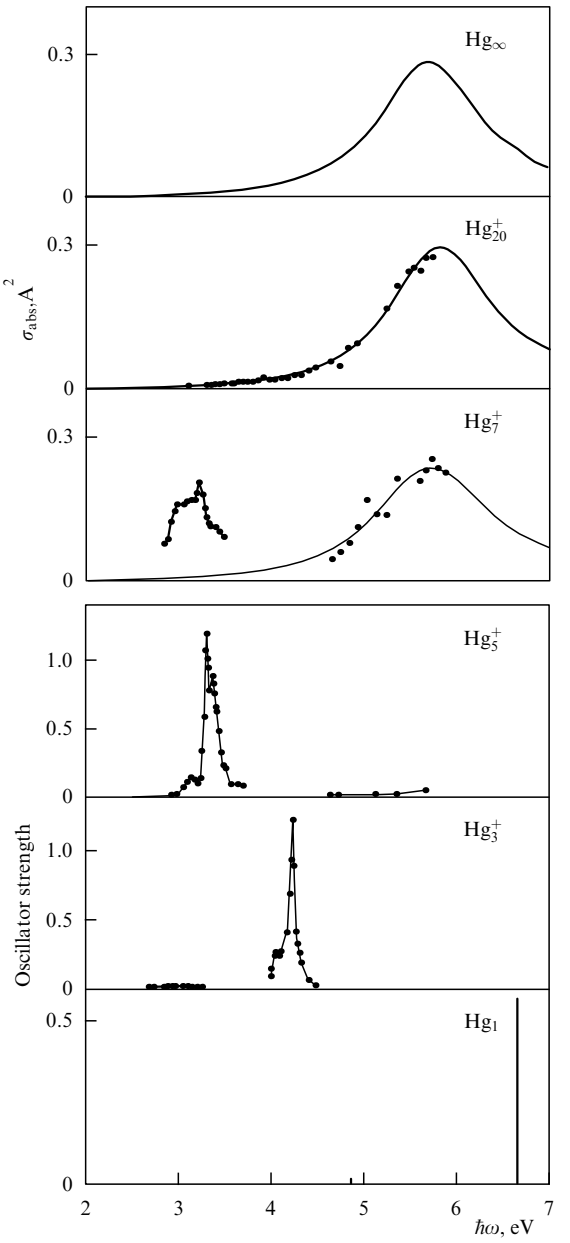

Figure 14. Absorption cross-section of mercury cluster ions [147, 148].

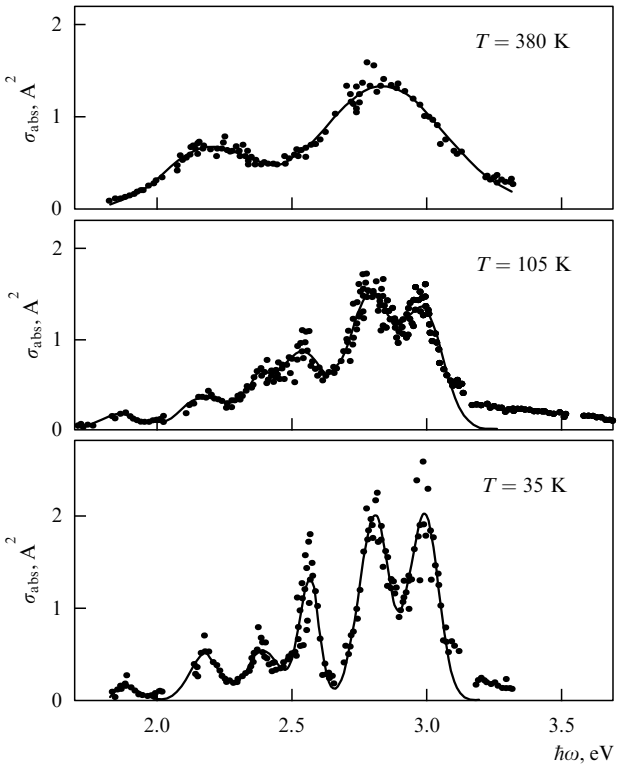

Figure 15. Absorption cross sections of Na_{11}^{-} cluster ions at different temperatures [149]: (a) $T = 380$ K, (b) $T = 105$ K, (c) $T = 35$ K.

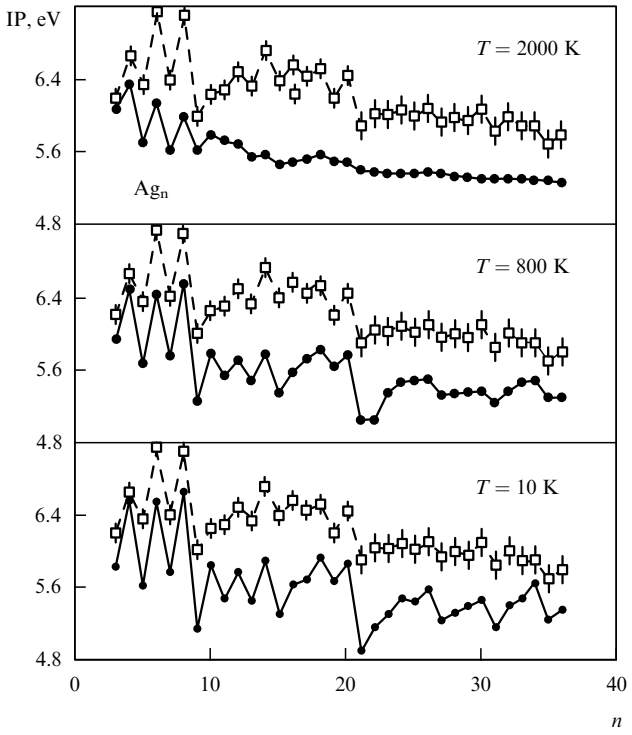

Figure 16. Ionization potential of silver clusters Ag_n at different temperatures according to calculations [150] (filled circles). Open squares correspond to experiment [151] at an unknown cluster temperature.

properties. Increasing the cluster temperature causes additional motion of nuclei and changes the cluster parameters. In particular, the dependence of cluster parameters on the number of cluster atoms becomes smoother with increasing temperature. This fact is demonstrated in Fig. 16 [150] where the ionization potential of silver clusters is given as a function of the number of cluster atoms at different temperatures.

As an atomic system, a metallic cluster admits saturation and nonlinear absorption of monochromatic power signals if the typical relaxation time of the excited states formed significantly exceeds the excitation time of the system [152]. Then alignment phenomena arise in the interaction of polarized monochromatic radiation with and atomic system, an a hole is burnt in the spectrum of this system. These phenomena were observed in experiments [153] with clusters Hg_7^{++} and Hg_9^{++} which were irradiated by polarized monochromatic light. Thus, metallic clusters can be used as a nonlinear optical element with a bleaching property under the action of monochromatic power pulses of light.

Thus, information the interaction of metallic clusters with electromagnetic waves testifies that these clusters have properties of atomic systems rather than bulk ones.

5.3 Absorption of films with embedded clusters

Let us consider the absorption of films of a transparent material with embedded clusters produced by the LECBD method [11 – 13]. Absorption in these films is determined by clusters which interact with an electromagnetic wave like free clusters. Assume the criterion

$$N\sigma_{\rm abs} r \ll 1\,, \tag{5.12}$$

to be valid, where N is the number density of clusters in the film, $\sigma_{\rm abs}$ is the cluster absorption cross section, and r is the cluster radius. Supposing clusters to be located randomly in the film and to interact independently with an electromagnetic wave, we have for the absorption coefficient k of the film:

$$k = N\sigma_{\rm abs}\,. \tag{5.13}$$

Here we consider embedded clusters as independent centres of absorption.

Figure 17 gives the absorption coefficient versus the photon energy for gold and indium clusters embedded in transparent matrices. One can see the validity of formula (5.13) in a rough approximation, so that the absorption coefficient is proportional to the cluster number density in the film. But a partial violation of this formula due to simultaneous interaction of an electromagnetic wave with several clusters could change the form of the absorption spectrum of films with increasing cluster number density.

A simultaneous interaction of an electromagnetic wave with many clusters takes place if they form a fractal structure as is shown in Fig. 18 [13]. Then a strong correlation in positions of neighbouring clusters in the film increases the absorption of an electromagnetic wave in comparison with a random distribution of clusters of the same number density. The absorption cross-section of a fractal aggregate with radius R small compared to the wavelength λ is expressed through the cross-section of absorption of an individual cluster by the formula [154, 155]:

$$\sigma = \sigma_{\rm abs}\left(\frac{R}{r}\right)^{3}, \tag{5.14}$$

where r is the cluster radius. Introducing the fractal dimensionality of the aggregate D, for the number of clusters

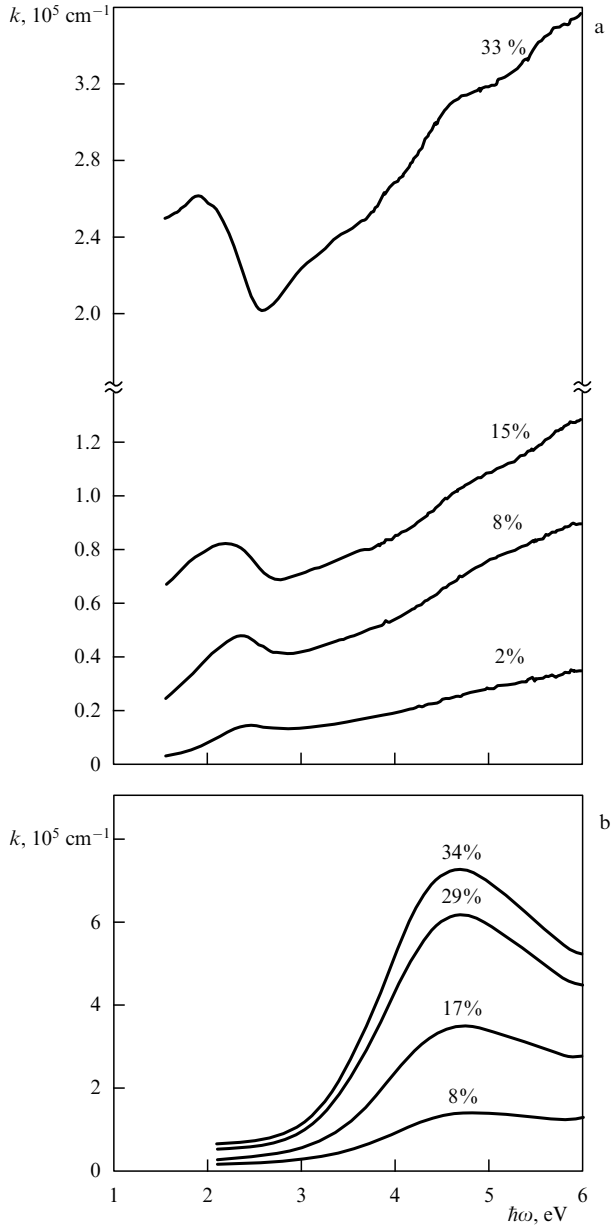

Figure 17. Absorption coefficient of films of thickness 50 nm with embedded clusters [13]. Volume fractions of clusters in the film are indicated; (a) a film of LiF with Au_{250} embedded clusters; (b) a film of MgF_2 with In_{1500} embedded clusters.

m constituting the fractal aggregate we have [156]

$$m = \left(\frac{R}{r}\right)^D . \tag{5.15}$$

If fractal aggregates are located randomly in a film and interact independently with an electromagnetic wave, we obtain for the absorption coefficient in the case when clusters form fractal aggregates with indicated parameters:

$$k = k_0 m^{3/D-1} , \tag{5.16}$$

where k_0 is the absorption coefficient of a film in which clusters of the same number density are distributed randomly and interact with an electromagnetic wave independently.

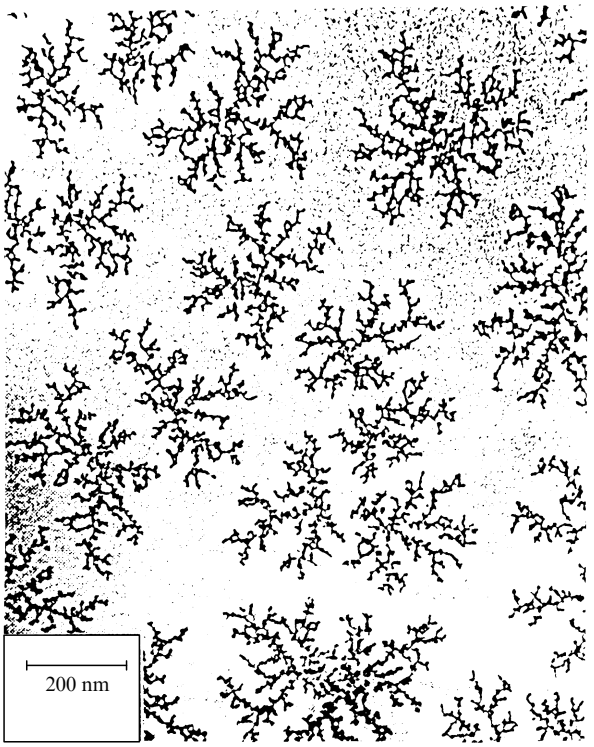

Figure 18. TEM (transverse electron microscopy) photograph of structures in a graphite film of thickness 0.5 nm with Sb_{2300} embedded clusters (diameter 5 nm) [13].

Formation of fractal aggregates in the regime of low-energy cluster beam deposition [13] is described by the model of deposition-diffusion aggregation [157]. According to this model, clusters roll on the surface until they join with another cluster or aggregate. Then they stop and form islands of clusters on the surface, and new clusters join these island-aggregates. Such a mechanism of aggregate growth is known as 'diffusion limited aggregation' [158]. The fractal dimensionality of the fractal aggregates formed in the two-dimensional case is approximately 1.7 [158–164], so that formula (5.16) has the form

$$k = k_0 m^{0.77} . \tag{5.17}$$

Thus, the formation of cluster structures resulting from deposition of solid clusters onto a surface leads to an increase of the absorption coefficient of the film formed.

5.4 Radiation of hot clusters

If clusters are located in a hot or weakly ionized gas, they are effective radiators and can determine the radiation of the system over a certain spectrum range. Let us use the principle of detailed balance in order to connect the spectral power of an individual cluster at a certain temperature with the absorption cross-section of this cluster. Then one can use the Kirchhoff law which establishes the connection between rates of absorption and emission of radiation. It gives for the spectral power of radiation

$$p(\omega) = \hbar\omega i(\omega)\sigma_{\text{abs}}(\omega) , \tag{5.18}$$

where

$$i(\omega) = \frac{\omega^2}{\pi^2 c^2}\left(\exp\frac{\hbar\omega}{T} - 1\right)^{-1} . \tag{5.19}$$

Here $i(\omega)$ is the random photon flux of black body radiation inside a space where this radiation propagates, so that $i(\omega)/4$ is the radiation flux from a surface of a bulk black body, and $\sigma_{\rm abs}(\omega)$ is the absorption cross-section for a small particle. Thus, we have for the spectral power of radiation of a small particle or cluster:

$$p(\omega) = \frac{\hbar\omega^3}{\pi^2 c^2}\,\sigma_{\rm abs}(\omega)\left(\exp\frac{\hbar\omega}{T} - 1\right)^{-1}. \qquad (5.20)$$

In particular, the radiation power of a small bulk particle of a radius r is

$$P = \int_0^\infty p(\omega)\,{\rm d}\omega = \frac{12\pi}{\hbar c}\,r^3 g\sigma T^5 \varkappa = \frac{46\pi r^3 g\sigma T^5}{\hbar c}\,, \quad \frac{Tr}{\hbar c} \ll 1\,, \qquad (5.21)$$

where we assume the value $g(\omega) = \varepsilon''\left[(\varepsilon'+2)^2 + (\varepsilon'')^2\right]^{-1}$ to be independent of the frequency, σ is the Stephan – Boltzmann constant, and the numerical coefficient $\varkappa = 3.83$. Thus, the radiation power $\sim T^5$ of a small particle differs from that of black body $\sim T^4$ corresponded to bulk systems.

According to formulas (5.3) and (5.10), the absorption cross-section of a cluster or small particle is proportional to the number of atoms n which constitute the cluster or small particle. From this it follows that the specific absorption cross-section, i.e. the cross-section per atom does not depend on the cluster size. Therefore the radiation power of particles per unit volume is proportional to the total number of atoms in particles which are located in the unit volume, or to the particle mass per unit volume. It does not depend on the distribution of particles by size if the particles have an identical form. Correspondingly, the total radiation power of a hot gas or plasma containing small particles or clusters is proportional to the total mass of particles in the volume where the radiation is created. This conclusion corresponds both to the spectral and total radiation power of the considered element of plasma. It is a general conclusion for a hot gas whose radiation is created by small particles [154, 165, 166]. This result follows both from the theory for bulk small particles and from the experiments for some metallic clusters.

Let us evaluate the parameters of radiation of a plasma with clusters or cluster ions. Use a simple model of cluster radiation by assuming parameters of hot clusters or cluster ions to be identical to that of Li, K and Ag-clusters [131 – 134]. Table 5 gives the specific powers of hot clusters:

$$P_{\rm rad} = \int \frac{p(\omega)\,{\rm d}\omega}{M}\,, \qquad (5.22)$$

where M is the cluster mass. We take the radiation power of a cluster ion to be proportional to its mass. Table 5 also lists the light efficiencies of hot tungsten cluster ions with the above model values for the absorption cross-sections. The light efficiency is determined by the formula

$$\eta = \frac{\int p(\omega)V(\omega)\,{\rm d}\omega}{\int p(\omega)\,{\rm d}\omega}\,, \qquad (5.23)$$

where $p(\omega)$ is given by formula (5.20), the function $V(\omega)$ characterizes the receptivity of the eye and has a maximum 683 lm W^{-1} at $\lambda = 555$ nm. For comparison Table 5 contains the light efficiencies of black body. Comparison of the data of

Table 5. Specific power of radiation ($P_{\rm rad}$) and efficiency of radiation (η) of large clusters. The specific power is expressed in 10^7 W g^{-1}, the light efficiency is given in parentheses and is expressed in lm W^{-1}. Data for the absorption cross-sections of Ag, K, and Li-clusters are used as model parameters for these temperatures.

Cluster	$P_{\rm rad}$ (η) at temperature					
	3000 K		3500 K		4000 K	
Ag	0.71	(51)	1.6	(75)	3.5	(88)
K	4.0	(108)	8.6	(141)	17	(165)
Li	2.0	(51)	4.9	(80)	10	(102)
Black body		(22)		(39)		(57)

Table 5 shows that the light efficiency for model metals is higher than that of black body because of the preferable absorption spectrum of the cluster ions (The infrared part is cut off in the spectrum of metallic cluster ions). Thus cluster ions in a discharge plasma provide a high radiation power per unit mass which is on average 1×10^8 W g^{-1} at $T = 3600$ K.

Thus, clusters or small particles introduced in a hot gas emit radiation and can be responsible for the radiation of the system. For example, this occurs in flames whose radiation is created by soot particles [165 – 167]. The same takes place in the products of combustion of solid fuels where small particles emit radiation. Below we consider one more example of this type when clusters are used as radiators in cluster sources of light.

6. Cluster plasma of light source

6.1 Processes in cluster plasma

According to its definition, a cluster plasma is an ionized gas containing clusters, so that clusters influence some plasma properties. Below we consider a discharge cluster plasma in which clusters are not of importance for an ionization equilibrium, but their radiation gives a significant contribution to the discharge power. This plasma is the basis of cluster sources of light. As follows from the analysis of Section 3.1, a significant number of clusters can exist only in a non-equilibrium plasma. Hence, the properties of a cluster plasma are determined by processes inside it which establish the specific character of equilibrium inside the plasma. Table 6 gives a list of these processes.

The effective interaction of metallic clusters with light and a profitable form of spectrum make metallic clusters effective radiators for a light source. Therefore, starting from the Weber and Scholl paper [168] of 1992, several types of cluster

Table 6. Processes in the cluster plasma of a light source.

Type of process	Process
Processes in arc plasma	Mobility of electrons
	Atom ionization by electron impact
	Three body recombination
	Drift of ions and electrons to walls
Kinetics of clusters	Evaporation of clusters
	Attachment of atoms to clusters
	Cluster collisions with electrons and atoms
Processes in atomic vapor	Ionization of vapor atoms
Processes with cluster ions	Ionization of clusters
	Diffusion and mobility of cluster ions
Chemical processes	Equilibrium of clusters and molecules

light sources were analyzed both by experimental and theoretical methods [168–173]. In all cases the clusters are located in a plasma. The first scheme of a cluster light source by Scholl and Weber [168] used tungsten and rhenium clusters in a 100 W microwave discharge. The important element of this scheme is a regenerative chemical cycle allowing gas at a low temperature and clusters at higher temperatures. For example, in the tungsten case the compound WO_2Br_2 was used at a pressure of approximately 1 atm which is a gas at low temperatures. Decomposition of WO_2Br_2 at temperatures 3000–4000 K leads to formation of WO_2 and W which can form clusters. Within the framework of this scheme a light efficiency for a cluster lamp of 56 lm W^{-1} was obtained in the tungsten case and 62 lm W^{-1} for the rhenium lamp. These values testify cheerful prospects for the above experiments so that they are now being developed.

Below we consider a cluster light source on the basis of an arc discharge in a cylindrical tube for supporting a cluster plasma (see Fig. 7). The peculiarities of this plasma allow us to simplify the scheme for a cluster light source. First, a high cluster temperature is required for optimal conditions of radiation, while the temperature of generation of clusters must be low. Then it is convenient to divide the region of generation of clusters and the region where they emit radiation. It is of importance that the temperature of clusters ranges between the electron and gaseous ones, and it tends to the electron temperature in the limit of a large electron number density. Separating the generation region from the discharge one by a grid leads to the cluster temperature in the generation region being equal to the gaseous temperature which is lower than the cluster temperature in the discharge region. Secondly, since clusters are positively charged in an arc discharge, they move towards the cathode under the action of discharge fields (the electrophoresis phenomenon). Hence, if the generation region is located near the anode, clusters propagate over all the discharge region. Clusters penetrating through a grid between the generation region and plasma obtain a charge and propagate over all the plasma. Simultaneously, they emit radiation because of the high temperature.

It is convenient to choose a refractory material for clusters in order to increase the temperature of radiating clusters, and an atomic gas with a small atomic ionization potential in order to avoid ionization of the vapor of the cluster material. Hence, we will choose xenon as a gas and tungsten as a cluster material, so that the optimal cluster temperature is 3000–3600 K. In addition the cluster plasma under consideration is a special physical object whose properties are determined by processes of a different kind represented in Table 6.

The generation of clusters proceeds in a special region as a result of conversion of an atomic vapor into a gas of clusters. This process was discussed in Section 3, and the best way to vaporize a solid material for its transformation into an atomic vapor is a gas discharge with sputtering of an electrode like the magnetron discharge [90–92] (see Section 3) which is operated at a higher pressure. Based on the data of cluster generation in magnetron discharge [90–92], below we take a typical size of clusters formed to be $n \sim 1000$.

Clusters introduced in the plasma are found in the ionization equilibrium with plasma electrons. If the electron temperature of the arc discharge is high enough, clusters have a positive charge. Note that the cluster charge is determined by the electron temperature of the arc discharge or by the typical energy of electrons in other gas discharges, because the cluster charge is established as a result of processes:

$$A_n^{+Z} + e \rightarrow A_n^{+Z+1} + 2e\,, \tag{6.1}$$

hence the cluster charge depends on the electron temperature only through the temperature dependence of the cluster ionization potential. Let us calculate the cluster charge Z. The probability $P_Z(n)$ that a cluster of n atoms has a charge Z satisfies a relation analogous to the Saha formula (2.17):

$$\frac{P_Z(n)N_e}{P_{Z+1}} = 2\left(\frac{m_e T_e}{2\pi\hbar^2}\right)^{3/2} \exp\left[-\frac{I_Z(n)}{T_e}\right], \tag{6.2}$$

where m_e, T_e are the electron mass and temperature, and $I_Z(n)$ is the ionization potential of cluster ions of charge Z consisting of n atoms. For large metallic clusters we have:

$$I_Z(n) = I_0(n) + \frac{Z^2e^2}{2r}\,,$$

where r is the cluster radius.

Let us write the ionization potential of a neutral cluster in the form

$$I_0(n) = W_0 + \frac{C}{n^{1/3}}\,,$$

where W_0 is the work function of the cluster material. In particular, in the tungsten case we have $W_0 = 4.4$ eV, and, if we assume this formula to be valid for a tungsten atom, one can obtain $C = 3.4$ 4eV. Thus the ionization potential of a cluster ion which has a charge Z and a large size is given by the formula:

$$I_Z(n) = W_0 + \frac{C}{n^{1/3}} + \frac{Z^2\gamma}{n^{1/3}}\,, \tag{6.3}$$

where $\gamma = e^2/(2r_W)$, and r_W is the Wigner–Seitz radius. In the tungsten case we have $\gamma = 5.3$ eV.

Let us define the mean charge of a cluster ion Z from the equality $P_{Z-1/2}(n) = P_{Z+1/2}(n)$. Then we have from formulae (6.2) and (6.3):

$$Z^2 = \frac{T_e}{\gamma}\ln\left[\frac{2}{N_e}\left(\frac{m_e T_e}{2\pi\hbar^2}\right)^{3/2}\right] - \frac{W_0}{\gamma} - \frac{C}{\gamma}\,. \tag{6.4}$$

Figure 19 gives the average cluster charge as a function of the electron temperature for tungsten and rhenium clusters of size $n = 1000$ at different electron number densities. From these data one can conclude that metallic clusters are charged in an arc plasma.

The cluster charge influences the processes involving clusters. Under the action of discharge electric fields charged clusters spread over the discharge tube. If clusters are introduced into arc through the anode, they move under the action of a discharge electric field towards to the cathode. This phenomenon is known as electrophoresis. In addition, the transverse electric field of a discharge sets clusters moving to the walls of the discharge tube. Hence, the lifetime of clusters in a gas discharge plasma is determined by their drift in the discharge tube. Let us estimate this time. One can calculate the mobility of clusters on the basis of the Chapman–Enskog approximation [174, 175] formula (2.27). This formula gives for the drift velocity of cluster ions in an

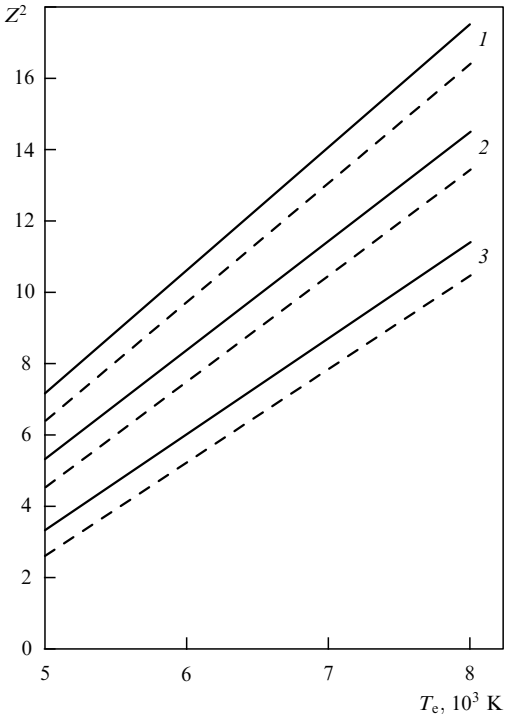

Figure 19. Mean charge of tungsten (solid curves) and rhenium clusters (dotted curve) as a function of the electron temperature at different number densities N_e of electrons: *1* — $N_e = 10^{13}$ cm^{-3}; *2* — $N_e = 10^{14}$ cm^{-3}; *3* — $N_e = 10^{15}$ cm^{-3}.

external electric field

$$v_{dr} = 1680 \frac{E}{N} Z \left(\frac{T}{1000} \right)^{1/2} \frac{1}{r_W^2 n^{2/3}} , \tag{6.5}$$

where the reduced electric field strength E/N is expressed in Td (1 Td $= 10^{-17}$ V cm^2), the gaseous temperature T is given in kelvin, and the Wigner – Seitz radius in A is the number density of xenon atoms in cm^{-3}. Because the charge of large clusters depends on the number of cluster atoms as $Z \sim n^{1/6}$, the drift velocity of large clusters varies with their size as $v_{dr} \sim n^{-1/2}$. In the case of tungsten clusters ($r_W = 1.36$ A) in an arc discharge of pressure 1 – 3 atm the drift velocity of clusters along the tube axis is about 5 cm s^{-1}.

6.2 Evolution of clusters in an arc plasma

In a cluster light source the region of cluster generation is separated from the plasma region, because a high cluster temperature in a plasma is not suitable for the generation of clusters. Therefore, clusters are introduced into a plasma and then partake in processes which lead to evaporation and growth of clusters. Because clusters in a hot gas or plasma are charged, processes of coagulation (4.1) are absent in their evolution. Below we consider the kinetics of clusters in a plasma and the evolution of the size distribution function of clusters in this plasma which develops on the basis of processes (2.22).

Processes of cluster growth and decay are determined by their interaction with the parent vapor which results from the evaporation of clusters. This interaction establishes the size distribution of clusters. If clusters are inserted into a hot gas, they partially evaporate and further interact with the forming atomic vapor as a result of processes (2.22):

$$A_n + A \leftrightarrow A_{n+1} . \tag{6.6}$$

Let f_n be the size distribution function of clusters, i.e. the number density of clusters consisting of n atoms. The kinetic equation for this function in a uniform gas has the form

$$\frac{\partial f_n}{\partial t} = I_{col}(f_n) , \tag{6.7}$$

where $I_{col}(f_n)$ is the collision integral. Below we get the expression for the collision integral taking into account processes (6.6) within the framework of the liquid drop model for clusters. The liquid drop model is suitable for large excited clusters, and according to this model, the binding energy of cluster atoms is determined by formula (2.1). On the basis of processes (6.6) we have for the collision integral:

$$I_{col}(f_n) = N k_{n-1} f_{n-1} - N k_n f_n - v_n f_n + v_{n+1} f_{n+1} . \tag{6.8}$$

Here N is the number density of free vapor atoms, v_n is the rate of atom evaporation from the surface of a cluster which is connected with the rate constant of atom attachment k_n by the principle of detailed balance [45, 46] and is given by formula (2.24):

$$v_{n+1} = k_n(T_{cl}) N_{sat}(T_{cl}) \exp \frac{\Delta\varepsilon}{T_{cl} n^{1/3}} . \tag{6.9}$$

Here T_{cl} is the cluster temperature, $N_{sat}(T_{cl})$ is the number density of atoms at the pressure of saturated vapor corresponding to the temperature T_{cl}. Note that this analysis admits different gaseous T and cluster T_{cl} temperatures, though it is not important for the nature of the processes. One can rewrite equation (6.8) on the basis of (6.9) in the form:

$$I_{col}(f_n) = -\frac{\partial}{\partial n} \left\{ k_0(T) \xi n^{2/3} \left[N f_n - N_{sat}(T_{cl}) \left(\frac{T_{cl}}{T} \right)^{1/2} \times \exp \left(\frac{\Delta\varepsilon}{T_{cl} n^{1/3}} \right) f_{n+1} \right] \right\} . \tag{6.10}$$

We use formula (2.10) for the attachment rate constant. Below for simplicity we take the gaseous T and cluster T_{cl} temperatures to be identical. Then the expression for the collision integral has the form:

$$I_{col}(f_n) = -\frac{\partial}{\partial n} \left\{ k_0(T) \xi n^{2/3} \times \left[N f_n - N_{sat}(T) \exp \left(\frac{\Delta\varepsilon}{T n^{1/3}} \right) f_{n+1} \right] \right\} . \tag{6.11}$$

The collision integral has the form of a flux in a space n and is responsible for transitions between clusters of different sizes. For large n, which are under consideration, the kinetic equation (6.7) takes the form of the Fokker – Planck equation. Using the relation $f_n = f_{n-1} + \partial f_n / \partial n$ for $n \gg 1$, one can represent the collision integral in the form of the sum of two fluxes, so that the first one, the hydrodynamic flux, is expressed through the first derivative over n, and the second flux, the diffusion one, includes the second derivative over n. The diffusion flux is small compared to the hydrodynamic

flux, but it is responsible for the width of the distribution function of clusters on sizes. Because under the conditions considered the width of the distribution function is determined by other processes, one can neglect the diffusion flux and represent the collision integral (6.11) in the form:

$$I_{\rm col}(f_n) = -\frac{\partial}{\partial n}\left\{k_0(T)\xi n^{2/3} f_n\left[N - N_{\rm sat}(T)\exp\left(\frac{\Delta\varepsilon}{Tn^{1/3}}\right)\right]\right\}. \tag{6.12}$$

Below we use this expression for the collision integral for the analysis of the size distribution function of clusters.

Let the clusters and their atomic vapor be located in a dense buffer hot gas or plasma like that described in the introduction. Then the processes of the cluster growth are faster than transport processes, so that one can consider that the evolution of the size distribution function of clusters proceeds in a uniform system. Because it is determined by processes (6.6), cluster growth takes place due to the interaction between clusters and their atomic vapor only. It is convenient to introduce the total number density of bound atoms in clusters

$$N_{\rm tot} = \sum_n n f_n\,, \tag{6.13}$$

so that the average cluster size is

$$\bar{n} = \sum_n \frac{n^2 f_n}{N_{\rm tot}}\,. \tag{6.14}$$

Under the conditions considered, the total number density of bound and free atoms is conserved

$$N + N_{\rm tot} = {\rm const}\,. \tag{6.15}$$

Then from the kinetic equation (6.7) and expression (6.12) for the collision integral it follows that the balance equation for the number density of free atoms is

$$\frac{{\rm d}N}{{\rm d}t} = -\frac{\rm d}{{\rm d}t}\sum_n n f_n = \int_0^\infty {\rm d}n\, k_0(T)\xi n^{2/3} f_n \times\left[N - N_{\rm sat}(T)\exp\left(\frac{\Delta\varepsilon}{Tn^{1/3}}\right)\right]. \tag{6.16}$$

The first term on the right-hand side of expressions (6.12) and (6.16) corresponds to the attachment of atoms to clusters, and the second term corresponds to the evaporation of atoms from the cluster surface. From this one can introduce the cluster critical size $n_{\rm c}$ for which the rates of these processes are:

$$N = N_{\rm sat}(T)\exp\left(\frac{\Delta\varepsilon}{Tn_{\rm c}^{1/3}}\right). \tag{6.17}$$

Note that the concept of a critical radius possesses a central place in the classical theory of condensation [4–7] where the number density of free atoms N do not vary in the course of condensation. Though in the case considered the number density of free atoms can vary and is supported by processes (6.6), the concept of the critical radius is a matter of principle. In particular, if the cluster size is smaller than the critical one, $I_{\rm col} > 0$, i.e. such clusters evaporate, while clusters grow if their size exceeds the critical one. This makes the cluster growth process not stationary in the absence of an external source and sink of clusters. Therefore we consider below the stationary size distribution function of clusters in presence of these processes. Then the kinetic equation for the distribution function has the form:

$$\frac{\partial f_n}{\partial t} = 0 = I_{\rm col}(f_n) + M_n - \frac{f_n}{\tau}\,. \tag{6.18}$$

Here M_n is the rate of generation of clusters, and τ is the cluster lifetime which is assumed to be independent of cluster size. Below we analyze this kinetic equation with expression (6.12) for the collision integral.

One can represent a general picture of the process. Part of the clusters grow, and the other part evaporates, so that clusters must be generated with sizes smaller and larger than the critical one. Hence, the number density of free atoms is determined by the function M_n. We consider such a regime when clusters reach large sizes compared to the critical one during their lifetime. This corresponds to a large value of the parameter

$$\beta = k_0 N\tau\xi \gg 1\,. \tag{6.19}$$

This parameter is large because it is the ratio of the kinetic rate $k_0 N\xi$ to the transport rate $1/\tau$, and transport processes are weak. Let us find the asymptotic solution of the kinetic equation (6.18) in the limit of large $n \gg n_{\rm c}$ if evaporation of large clusters is not essential, i.e. $N \gg N_{\rm sat}(T)$ or $\Delta\varepsilon \gg Tn_{\rm c}^{1/3}$. Then the kinetic equation has the form

$$\frac{{\rm d}(n^{2/3} f_n)}{{\rm d}n} + \frac{f_n}{\beta} = 0 \tag{6.20}$$

and its solution is

$$f_n = C\frac{\exp(-3n^{1/3}/\beta)}{n^{2/3}}\,, \qquad n \gg n_{\rm c}\,. \tag{6.21}$$

Let us find the average cluster size supposing that it is determined by large clusters. On the basis of formulae (6.14) and (6.21) we have

$$\bar{n} = \frac{80}{81}\frac{C\beta^7}{N_{\rm tot}}\,, \qquad n_{\rm c} \ll \beta^3\,.$$

If we assume that large clusters give the main contribution to the normalization condition (6.13) of the size distribution function, we get

$$N_{\rm tot} = \frac{2}{9}\,C\beta^4\,, \qquad \bar{n} = \frac{40}{9}\,\beta^3\,. \tag{6.22}$$

This dependence can be obtained from the equation of cluster growth if we neglect the evaporation of clusters

$$\frac{{\rm d}n}{{\rm d}t} = k_0 N\xi n^{2/3}\,.$$

The solution of this equation is

$$n = \left(\frac{k_0 N\xi t}{3}\right)^3,$$

and the change of time t by the cluster lifetime τ in a plasma gives the estimate $n \sim \beta^3$ which coincides with (6.22).

Let us construct the size distribution function of clusters in the case $n_{\rm c}^{1/3} \ll \Delta\varepsilon/T$ if the rate of evaporation of large

clusters is small compared to the rate of their growth owing to the attachment of atoms. Then we use the asymptotic expression (6.21) for the size distribution function of clusters and for small clusters we account for the equality between rates of the evaporation and attachment processes. This equality follows from equation (6.16) since the distribution is stationary. We suppose the total rate of attachment is determined by large clusters with the size distribution function (6.21), so that the above condition has the form

$$\int_0^\infty n^{2/3} f_n \, \mathrm{d}n \exp\left(\frac{\Delta\varepsilon}{Tn^{1/3}}\right) = \frac{2}{9} C\beta^3 S . \tag{6.23}$$

Here $S = N/N_{\mathrm{sat}}(T)$ is the degree of supersaturation, and in the current regime $S \gg 1$. Note that small clusters $n \sim n_{\mathrm{c}}$, $n \ll \beta^3$ give the main contribution into the integral of the left-hand side of (6.23). It is convenient to represent the size distribution function in the form

$$f_n = C \exp\left(-\frac{a}{n} - \frac{3n^{1/3}}{\beta}\right) \frac{1}{n^{2/3}} . \tag{6.24}$$

In such a form the distribution function transforms to (6.21) in the limit of large sizes, and integral (6.23) converges at small cluster sizes. The parameter a can be found from relation (6.23). Supposing that this integral converges in a narrow region of a, we get

$$a = 0.34(\beta^2 S)^{4/7} \left(\frac{\Delta\varepsilon}{T}\right)^{9/7} . \tag{6.25}$$

From this it follows $a \gg 1$, and this parameter is connected with the critical cluster size. For this form of the distribution function, large cluster sizes give the main contribution to the normalization condition, so that on the basis of (6.22) $N_{\mathrm{tot}} = 2C\beta^4/9$ one can transform formula (6.24) to the form:

$$f_n = \frac{9N_{\mathrm{tot}}}{2\beta^4 n^{2/3}} \exp\left(-\frac{a}{n} - \frac{3n^{1/3}}{\beta}\right) . \tag{6.26}$$

Formulas (6.25) and (6.26) are valid for $S \gg 1$ or $n_{\mathrm{c}} \ll (\Delta\varepsilon/T)^3$. But the method of deduction of these expressions shows that the size distribution function can be obtained by a numerical solution of equation (6.18) for any relation between parameters.

Let us analyze the conservation laws which follow from the kinetic equation (6.18) for the generation function M_n. First, due to the form of the collision integral this equation gives the following integral relation

$$\int_0^\infty M_n \, \mathrm{d}n = \int_0^\infty f_n \frac{\mathrm{d}n}{\tau} . \tag{6.27a}$$

which means the equality of rates of formation and loss for a number of clusters. The other relation accounts for the stationary process. Then from relation (6.16) it follows

$$\int_0^\infty n I_{\mathrm{col}}(f_n) \, \mathrm{d}n = 0 ,$$

and equation (6.18) gives the integral relation

$$\int_0^\infty M_n n \, \mathrm{d}n = \frac{N_{\mathrm{tot}}}{\tau} . \tag{6.27b}$$

This means an equality of rates of generation and loss of numbers of bound atoms.

One more relation follows from relation (6.27a) by dividing it into two parts. Indeed, let us divide a system of clusters into two subsystems, so that the first one contains small clusters of size $n < n_{\mathrm{c}}$, and the second consists of large clusters with $n > n_{\mathrm{c}}$. Because small clusters evaporate and large ones grow, direct transitions between clusters of the two subsystems are absent. This fact takes a mathematical form if we integrate the kinetic equation (6.18) over clusters of each subsystem:

$$\int_0^{n_{\mathrm{c}}} M_n \, \mathrm{d}n = \int_0^{n_{\mathrm{c}}} f_n \frac{\mathrm{d}n}{\tau} , \qquad \int_{n_{\mathrm{c}}}^\infty M_n \, \mathrm{d}n = \int_{n_{\mathrm{c}}}^\infty f_n \frac{\mathrm{d}n}{\tau} . \tag{6.28}$$

Relations (6.28) indicate the connection between the value of the critical size n_c and the spectra of generating clusters M_n. Relations (6.27) and (6.28) follow from the kinetic equation (6.18) and reflect some physical peculiarities of the kinetics of the cluster processes. They can be used for their analysis.

From the above analysis follow the expressions for the size distribution function of clusters located in a cluster plasma for some regime of their kinetics. Numerical evaluations on the basis of the collision integral (6.12) for cluster kinetics, the kinetic equation (6.18) and physical peculiarities of kinetics (6.27) can give such results for certain regimes of the cluster kinetics.

6.3 Typical parameters of cluster plasma

Let us estimate typical parameters of the cluster plasma under consideration. The character of evolution of a cluster size is determined by the equilibrium between clusters and the vapor resulting from their evaporation. Above we consider the kinetics of evolution of the size distribution function of clusters, and now note that the equilibrium between clusters and their atomic vapor is, actually, the equilibrium between free and bound atoms. In the regime under consideration the number density of free atoms is small compared to the number density of bound atoms, and the total number density of free and bound atoms is significantly less than the number density of atoms of the buffer gas. But the number density of free atoms of an evaporated material several times exceeds the saturated vapor number density at a given temperature that results from the condition of the finite value of the critical cluster size. Hence, the cluster temperature is restricted. In the case of tungsten clusters the limit of the cluster temperature is 3600 – 3800 K.

The electron temperature of this arc discharge is restricted to a value of about 6000 K. Indeed, due to the ionization process the following ionization equilibrium is established (for definiteness, we consider tungsten as a cluster material):

$$\mathrm{W} + \mathrm{e} \leftrightarrow \mathrm{W}^+ + 2\mathrm{e} \tag{6.29}$$

Along with a parent atomic vapor, clusters must support a gas of atomic ions. At indicated temperatures the contribution of tungsten atomic ions to the total number density of free atoms and atomic ions does not exceed 10%. The gaseous temperature is such that the cluster temperature which is determined by formula (2.18) lies in the range 3000 – 3600 K. The gaseous temperature lies in the limits 1000 – 2500 K.

The parameters of a xenon arc discharge of high pressure [176, 177] which is the basis of a cluster plasma of a light source must correspond to the above parameters. A typical electric field strength E/N is about 0.02 Td at a xenon

pressure of 1–3 atm, and the specific power of discharge is 20–40 W cm^{-1}. The contraction of this gas discharge [176, 177] is principle. In the considered regime the current cross-section is several times less than the total cross-section of the discharge tube.

In order to analyze the character of cluster growth in the considered regime, let us take typical parameters of the arc discharge plasma. Let us take the electron temperature as $T_e = 5600$ K, the gaseous temperature as $T = 2000$ K and the xenon pressure as $p = 3$ atm. Then the current radius is 0.4 cm, the specific power is about 30 W cm^{-1}, while the density power at the discharge axis is about 200 W cm^{-3}, and the cluster temperature according to formula (2.17) is $T_{cl} = 3200$ K. In the region of cluster generation (see Fig. 7) the cluster temperature coincides with the gaseous one which we take as $T = 2000$ K. The number density of tungsten atoms at this temperature is $N_{sat} = 5 \times 10^4$ cm^{-3} at the saturated vapor pressure and $N = 5 \times 10^6$ cm^{-3} for clusters with the critical size $n = 10^3$. The cluster temperature in the arc region $T_{cl} = 3200$ K corresponds to the atom number density $N = 2.4 \times 10^{13}$ cm^{-3} for this critical size. It is the number density of free atoms resulting from evaporation of clusters of this size, and the number density of bound atoms in clusters exceeds this value significantly. Hence, the cluster plasma under consideration exists only at high rates of generation of atomic vapor as a result of vaporization of bulk material.

Under the considered conditions, the drift time of clusters from the axis through the current region is $\tau \sim 0.4$ s. This is the lifetime of clusters in this plasma. Note that a typical time of atom attachment to a cluster is ~ 2 μs, that is small compared to the cluster drift time through the plasma region. Since the rate constant of atom attachment for tungsten clusters is $k_0 = 3.7 \times 10^{-11}$ cm^3 s^{-1}, we have for parameter (6.19) $\beta \sim 400$, and the mean cluster size $\bar{n} \sim 2 \times 10^8$ according to formula (6.22). Though such clusters have a small radius (~ 0.2 μm) compared to a typical wavelength, the kinetics of cluster growth must be revised for such large clusters. Nevertheless, these estimates show the formation of large clusters in the plasma region.

The cluster plasma under consideration provides a light efficiency of approximately 50 lm W^{-1} that follows both from experiment [168] and theory [174]. Though this value is lower than that of gas discharge lamps (100 lm W^{-1}), cluster lamps have some advantages due to a low heat tension. Hence, cluster light sources are profitable for power lamps.

The considered scheme of tungsten conversion consists in the formation of an atomic vapor as a result of sputtering of a bulk material and the formation of clusters from vapor atoms. The clusters are then directed to a plasma where they are used as radiators. In the end the clusters attach to the walls of the discharge tube. Thus, this scheme leads to tungsten consumption. In the above example the tungsten consumption is about 1 μg/(cm s), when the light intensity is approximately 1000 lm W^{-1}.

There is a more profitable method of tungsten usage [168–172]. At low temperatures tungsten is found in the compound WO_2Br_2, and at high temperatures this compound decays, and tungsten oxides join in clusters if the cluster temperature is not very high. This method combines well with a contact gas discharge because in this case an ion current does not go through the main part of the volume. Though this scheme is preferable to the considered one, we cannot analyze it because of the absence of information for tungsten oxides.

Thus, the cluster plasma under consideration, which is the basis of cluster light sources, is a specific physical object. Its properties are determined by processes involving both plasma charged particles and clusters. The electrical parameters of the plasma do not depend on the absence of clusters, while the clusters determine the radiation of the plasma which powerful is compared with the total discharge power. The peculiarity of the plasma is the requirement of a high rate of cluster generation, so that the existence of the cluster plasma is characterized by a threshold. On the other hand, the contribution of cluster radiation to the total discharge power can not exceed a certain value, otherwise a discharge instability can develop. The existence of clusters in a discharge plasma is accompanied by processes of cluster growth resulting from the interaction with their own vapor. Thus, the cluster plasma of light sources is a special physical object which has a significance both fundamentally and in application.

7. Conclusions

The research of cluster beams, cluster assembled materials and cluster plasmas is in progress. These could be the basis of fine new technologies. It is of principle that these systems involving clusters are non-equilibrium ones, so that their properties are determined by the processes inside them. Hence, cluster applications require a detailed study of the processes involving clusters and that is the topic of this paper.

References

1. Echt O, Sattler K, Recknagel E *Phys. Rev. Lett.* **47** 1121 (1981)
2. Harris I A, Kidwell R S, Northby J A *Phys. Rev. Lett.* **53** 2390 (1984)
3. Knight W D et al. *Phys. Rev. Lett.* **52** 2141 (1984)
4. Zel'dovich Ja B *Zh. Eksp. Teor. Fiz.* **12** 525 (1942)
5. Frenkel Ja I *Kinetic Theory of Liquids* (Oxford: Oxford University Press, 1946)
6. Abraham F F *Homogeneous Nucleation Theory* (New York: Academic Press, 1974)
7. Landau L D, Lifshitz E M *Statistical Physics* Vol. 2. (Oxford, Pergamon Press, 1980)
8. Becker E W, Bier K, Henkes W *Z. Phys.* **146** 333 (1956)
9. Henkes W *Z. Naturforsch. A* **16** 842 (1961)
10. Henkes W *Z. Naturforsch. A* **17** 786 (1962)
11. Fuchs G et al. *Phys. Rev. B* **44** 3926 (1991)
12. Melinon P et al. *Int. J. Mod. Phys. B* **9** 339 (1995)
13. Peres A et al. *J. Phys. D* **30** 709 (1997)
14. Morokhov I D, Trusov L I, Lapovok V N *Fizicheskie Yavleniya v Ul'tradispersnykh Sredakh* (Physical Phenomena in Ultradispersive Mixtures) (Moscow: Energoatomizdat, 1984)
15. Miehle W et al. *J. Chem. Phys.* **91** 5940 (1989)
16. Martin T P et al. *Chem. Phys. Lett.* **176** 343 (1991)
17. Näher U, Zimmermann U, Martin T P *J. Chem. Phys.* **99** 2256 (1993)
18. Martin T P et al. *Chem. Phys. Lett.* **172** 209 (1990)
19. Hoare M R, Pal P *Adv. Phys.* **20** 161 (1971); **24** 645 (1975)
20. Hoare M R *Adv. Chem. Phys.* **40** 49 (1979)
21. Hoare M R, McInnes J A *Adv. Phys.* **32** 791 (1983)
22. Farges J et al. *Surf. Sci.* **106** 95 (1981)
23. Lee J W, Stein G D *J. Phys. Chem.* **91** 2450 (1987)
24. Raoult B et al. *Philos. Mag. B* **60** 881 (1989)
25. Van der Waal B W *J. Chem. Phys.* **90** 3407 (1989)
26. Northby J A et al. *Z. Phys. D* **12** 69 (1989)
27. Raoult B et al. *Z. Phys. D* **12** 85 (1989)
28. Xie J et al. *J. Chem. Phys.* **91** 612 (1989)
29. Poye J P K, Berry R S *J. Chem. Phys.* **103** 4234 (1995)
30. Ino S *J. Phys. Soc. Jpn.* **27** 941 (1969)
31. Lide D R (Ed.) *Handbook of Chemistry and Physics*, 74th ed (London: CRC Press, 1993–1994)

32. Smirnov B M, Yatsenko A S *Usp. Fiz. Nauk* **166** 225 (1996) [*Phys. Usp.* **39** 211 (1996)]
33. Smirnov B M *Usp. Fiz. Nauk* **162** 119 (1992) [*Phys. Usp.* **35** 37 (1992)]
34. Smirnov B M *Usp. Fiz. Nauk* **163** (10) 29 (1993) [*Phys. Usp.* **36** 933 (1993)]
35. Smirnov B M *Phys. Scripta* **52** 710 (1995)
36. Northby J A *J. Chem. Phys.* **87** 6166 (1987)
37. Smirnov B M *Phys. Scripta* **53** 613 (1996)
38. Von Helden G et al. *J. Chem. Phys.* **95** 3895 (1991)
39. Jarrold M F, Constant V A *Phys. Rev. Lett.* **67** 2994 (1991)
40. Jarrold M F, Bower J E *J. Chem. Phys.* **96** 9180 (1992)
41. Jarrold M F, Bower J E *J. Chem. Phys.* **98** 2399 (1993)
42. Landau L D, Lifshitz E M *Mechanics* (Oxford: Pergamon Press, 1976)
43. Landau L D, Lifshitz E M *Statistical Physics* Vol. 1 (Oxford: Pergamon Press, 1980)
44. Smirnov B M *Phys. Scripta* **51** 380 (1995)
45. Smirnov B M *Plasma Chem. Plasma Processes.* **13** 673 (1993)
46. Smirnov B M *Usp. Fiz. Nauk* **164** 665 (1994) [*Phys. Usp.* **37** 621 (1994)]
47. Lifshitz E M, Pitaevskiĭ L P *Physical Kinetics* (Oxford, NY: Pergamon Press, 1981)
48. Hagena O F, in *Molecular Beams and Low Density Gas Dynamics* (Ed. P P Wegener) (New York: Dekker, 1974) p. 93
49. Takagi T *Pure Appl. Chem.* **60** 781 (1988)
50. Becker E W *Laser Part. Beams* **7** 743 (1989)
51. Hagena O F *Rev. Sci. Instrum.* **36** 2374 (1992)
52. Takagi T *J. Vac. Sci. Technol. A* **2** (2) 382 (1984)
53. Gspann J, in *Physics and Chemistry of Finite Systems: From Clusters to Crystals* Vol. 2 (Eds P Jena, R K Rao, S N Khanna) (Dordrecht, Amsterdam: Kluwer Acad. Publ., 1992) p. 1115
54. Hagena O F, Knop G, Ries R *KfK Nachr.* **23** 136 (1991)
55. Hagena O F, Knop G, Linker G, in *Physics and Chemistry of Finite Systems: From Clusters to Crystals* Vol. 2 (Eds P Jena, R K Rao, S N Khanna) (Dordrecht, Amsterdam: Kluwer Acad. Publ., 1992)
56. Henkes P R W, Klingelhofer R *J. Physique* **50** 159 (1989)
57. Henkes P R W, Klingelhofer R *Vacuum* **39** 541 (1989)
58. Gspann J *Z. Phys. D* **26** S174 (1993)
59. Hagena O F *Surf. Sci.* (106) 101 (1981)
60. Hagena O F, Knop G, in *Proc. 18th GRD Symposium* (Vancouver, Canada, 1992)
61. Hagena O F *Z. Phys. D* **4** 291 (1987)
62. Hagena O F *Z. Phys. D* **17** 157 (1990)
63. Hagena O F *Z. Phys. D* **20** 425 (1991)
64. Hagena O F, Obert W *J. Chem. Phys.* **56** 1793 (1972)
65. Gspann J *Z. Phys. D* **3** 143 (1986)
66. Gspann J *Z. Phys. D* **20** 421 (1991)
67. Sattler K, Muhlbach J, Recknagel E *Phys. Rev. Lett.* **45** 821 (1980)
68. Kappes M M, Kunz R W, Schumacher E *Chem. Phys. Lett.* **91** 413 (1982)
69. Takagi T *Pure Appl. Chem.* **60** 781 (1988)
70. Martin T P *J. Chem. Phys.* **81** 4426 (1984)
71. Castleman A W, Keesee R G *Z. Phys. D* **3** 167 (1986)
72. Smalley R E *Laser Chem.* **2** 167 (1983)
73. Hopkins J P et al. *J. Chem. Phys.* **78** 1627 (1984)
74. Liu Y et al. *J. Chem. Phys.* **85** 7434 (1986)
75. Milani P, de Heer W A *Rev. Sci. Instrum.* **61** 1835 (1990)
76. Cheshnovsky O et al. *Chem. Phys. Lett.* **138** 119 (1987); *Rev. Sci. Instrum.* **58** 2131 (1987)
77. Begemann W et al. *Z. Phys. D* **3** 183 (1986)
78. Gantefor G et al. *Z. Phys. D* **9** 253 (1988)
79. Gantefor G et al. *J. Chem. Soc. Faraday Trans.* **86** 2483 (1990)
80. Lutz H O, Melwes-Broer K H *Nucl. Instrum. Methods Phys. Res. B* **59** 395 (1991)
81. Barlak T M et al. *J. Phys. Chem.* **85** 3840 (1981)
82. Barlak T M et al. *J. Am. Phys. Soc.* **104** 1212 (1982)
83. Ens W, Beavis R, Standing K G *Phys. Rev. Lett.* **50** 27 (1983)
84. Martin T P *Phys. Rep.* **95** 167 (1983)
85. Martin T P *Ber. Bunsen-Ges. Phys. Chem.* **88** 300 (1984)
86. Fayet P, Woste L *Z. Phys. D* **3** 177 (1986)
87. Begemann W et al. *Z. Phys. D* **12** 229 (1989)
88. Mesyats G A *Éktony* Ch. 1(Ectons) Pt. 1 (Ekaterinburg: Nauka, 1993)
89. Mesyats G A *Usp. Fiz. Nauk* **166** (6) 601 (1995) [*Phys. Usp.* **38** 567 (1995)]
90. Haberland H et al. *J. Vac. Sci. Technol. A* **10** 3266 (1992)
91. Haberland H et al. *Mater. Sci. Eng. B* **19** 31 (1993)
92. Haberland H et al. *J. Vac. Sci. Technol. A* **12** 2925 (1994)
93. Haberland H et al. *Surf. Rev. Lett.* **9** 887 (1993)
94. Haberland H, Insepov Z, Moseler M *Z. Phys. D* **26** 229 (1993)
95. Haberland H, Insepov Z, Moseler M *Phys. Rev. B* **51** 11061 (1995)
96. Beuhler R J, Friedlander G, Friedman L *Phys. Rev. Lett.* **63** 1292 (1989)
97. Leonas V B *Usp. Fiz. Nauk* **160** (11) 135 (1990) [*Sov. Phys. Usp.* **33** 956 (1990)]
98. Beuhler R J et al. *Phys. Rev. Lett.* **67** 473 (1991)
99. Beuhler R, Friedman L *Chem. Rev.* **86** 521 (1986)
100. Matthew M W et al. *J. Phys. Chem.* **90** 3152 (1986)
101. Gleiter H *Nanostruct. Mater.* **6** 3 (1995)
102. Takagi T *Cluster Beam Deposition and Epitaxy* (New York, Parker Ridge: Noyes Publications, 1988)
103. Takagi T, Yamada I, Sabaki A *J. Vac. Sci. Technol.* **12** 1228 (1979)
104. Yamada I, Usui H, Takagi T *J. Phys. Chem.* **91** 2463 (1980)
105. Yamada I, Inokawa H, Takagi T *J. Appl. Phys.* **56** 2746 (1984)
106. Takaoka H, Yamada I, Takagi T *J. Vac. Sci. Technol. A* **3** 2665 (1985)
107. Takagi T et al. *Thin Solid Films* **126** 149 (1985)
108. Usui H, Yamada I, Takagi T *J. Vac. Sci. Technol. A* **4** 52 (1986)
109. Yamada I et al. *J. Vac. Sci. Technol. A* **4** 722 (1986); Sosnowski M, Yamada I *Nucl. Instrum. Methods Phys. Res. B* **46** 397 (1990)
110. Takagi T *Vacuum* **36** 27 (1986)
111. Huq S E, McMahon R A, Ahmed H *Semicond. Sci. Technol.* **5** 771 (1990)
112. Takaoka H, Ishikawa J, Takagi T *J. Vac. Sci. Technol. A* **8** 840 (1990)
113. Sosnowski M, Usui H, Yamada I *J. Vac. Sci. Technol. A* **8** 1470 (1990)
114. McEachern R L et al. *J. Vac. Sci. Technol. A* **9** 3105 (1991)
115. Jena P et al. *Mater. Res. Soc. Symp. Proc.* **206** 3 (1991)
116. Khanna S N, Jena P *Phys. Rev. Lett.* **69** 1664 (1992)
117. De Heer W A, Milani P, Chatelain A *Phys. Rev. Lett.* **65** 488 (1990)
118. Khanna S N, Linderoth S *Phys. Rev. Lett.* **67** 742 (1991)
119. Wiel R *Z. Phys. D* **27** 89 (1993)
120. Smirnov B M, Strizhev A Yu *Phys. Scripta* **49** 615 (1994)
121. Smirnov B M *Phys. Scripta* **50** 364 (1994)
122. Valkealahti S, Manninen M *Phys. Rev. B* **50** 17564 (1994)
123. Khatoun J et al. *Z. Phys. D* **34** 47 (1995)
124. Rao B K, Smirnov B M *Phys. Scripta* **56** 439 (1997)
125. Haberland H, Buck U, Tolle M *Rev. Sci. Instrum.* **56** 1712 (1985)
126. Preuss D R, Pace S A, Gole J L *J. Chem. Phys.* **71** 3553 (1979)
127. Landau L D,Lifshitz E M *Electrodynamics of Continuous Media* (Oxford: Pergamon Press, 1960)
128. Mie G *Ann. Phys.* **25** 377 (1908)
129. Kittel Ch *Introduction to Solid State Physics* 6th ed. (New York: Wiley and Sons, 1986)
130. Ashcroft N W, Mermin N D *Solid State Physics* (New York: Holt, Rinehart and Winston, 1976)
131. Teggesbaumker J et al. *Chem. Phys. Lett.* **190** 42 (1992)
132. Brechignac C et al. *Chem. Phys. Lett.* **164** 433 (1989)
133. Brechignac C et al. *Phys. Rev. Lett.* **68** 3916 (1992)
134. Brechignac C et al. *Phys. Rev. Lett.* **70** 2036 (1993)
135. Alexander M L et al. *Phys. Rev. Lett.* **57** 976 (1986)
136. Brechignac C et al. *Chem. Phys. Lett.* **189** 28 (1992)
137. Krainov V P, Reiss H B, Smirnov B M *Radiative Transitions in Atomic Physics* (New York: Wiley, 1987)
138. Radzig A A, Smirnov B M *Reference Data on Atoms, Molecules, and Ions* (Berlin: Springer-Verlag, 1985)
139. Ekardt W *Phys. Rev. B* **31** 6360 (1985)
140. Kresin V *Phys. Rev. B* **39** 3042 (1989); **40** 12507 (1989); **42** 3247 (1990)
141. Yannouleas C et al. *Phys. Rev. Lett.* **63** 255 (1989)
142. Serra Ll et al. *Phys. Rev. B* **39** 8247 (1989)
143. Bonacic-Koutecky, Fantucci P, Kountecky J *J. Chem. Phys.* **93** 3802 (1990)

144. Ekardt W, Penzar Z *Phys. Rev. B* **43** 1322 (1991)
145. Selby K et al. *Z. Phys. D* **19** 41 (1991)
146. Blundell S A, Guet C *Z. Phys. D* **28** 81 (1993)
147. Haberland H et al. *Phys. Rev. Lett.* **69** 3212 (1992)
148. Haberland H et al. *Z. Phys. D* **26** 8 (1993)
149. Haberland H, von Issendorff B *Phys. Rev. Lett.* **76** 1445 (1996)
150. Yannouleas C, Landman U *Phys. Rev. Lett.* **78** 1424 (1997)
151. Jackschath C et al. *Z. Phys. D* **22** 517 (1992)
152. Demtröder W *Laser Spectroscopy: Basic Concepts and Instrumentation* (Berlin: Springer-Verlag, 1996)
153. Schmidt M et al. *Phys. Rev. Lett.* (in press)
154. Smirnov B M *Usp. Fiz. Nauk* **163** (7) 51 (1993) [*Phys. Usp.* **36** 592 (1993)]
155. Smirnov B M *Int. J. Theor. Phys.* **32** 1453 (1993)
156. Mandelbrot B *The Fractal Geometry of Nature* (San Francisco: Freeman, 1982)
157. Jensen P et al. *Phys. Rev. B* **50** 15316 (1994)
158. Witten T A, Sander L M *Phys. Rev. Lett.* **47** 1400 (1981)
159. Meakin P *Phys. Rev. A* **27** 604, 1495 (1983); **27** 604 (1983)
160. Meakin P *J. Chem. Phys.* **79** 2426 (1983)
161. Racz Z, Plischke M *Phys. Rev. A* **31** 985 (1985)
162. Sahimi M et al. *Phys. Rev. A* **32** 590 (1985)
163. Ball R C *Physica A* **140** 62 (1986)
164. Meakin P et al. *Phys. Rev. A* **35** 5233 (1987)
165. Luizova L A, Smirnov B M, Khakhaev A D *Dokl. Akad. Nauk SSSR* **34** 1359 (1989) [*Sov. Phys. Dokl.* **34** 1086 (1989)]
166. Luizova L A et al. *Teplofiz. Vys. Temp.* **28** 897 (1990) [*High Temp.* **28** 674 (1990)]
167. Faradey M *The Chemical History of a Candle* (New York: Crowell, 1957)
168. Weber B, Scholl R *J. Illum. Eng. Soc.* (Summer 1992) p. 93
169. Scholl R, Weber B, in *Physics and Chemistry of Finite Systems: from Clusters to Crystals* Vol. 2 (Eds P Jena, S N Khana, B K Rao) (Dordrecht: Kluwer Academic Publ., 1992) p. 1275
170. Weber B, Scholl R *J. Appl. Phys.* **74** 607 (1993)
171. Scholl R, Natour G, in *Phenomena in Ionized Gases* (Eds K H Becker, W E Carr, E E Kunhardt) (Woodbury: AIP Press, 1996) p. 373
172. Chapman S, Cowling T G *The Mathematical Theory of Non-Uniform Gases* (Cambridge: Cambridge University Press, 1952)
173. Ferziger J H, Kaper H G *Mathematical Theory of Transport Processes in Gases* (Amsterdam: North-Holland, 1972)
174. Eletskiĭ A V, Smirnov B M *Usp. Fiz. Nauk* **166** 1197 (1996) [*Phys. Usp.* **39** 1137 (1996)]
175. Smirnov B M, Smirmov M B *Physica Scripta* **56** 302 (1997)